J. Webster (ed.), *Wiley Encyclopedia of Electrical and Electronics Engineering*

HUMAN MOTION ANALYSIS

Human locomotion is an acquired yet complex behavior requiring little thought during routine activities. It involves the integration of intricate signals from the nervous system, which result in muscle contraction and subsequent joint movement. Our comprehension of the development of coordinated gait activity, however, remains enigmatic despite numerous and profound advances in technology. The quest for knowledge in this field challenges various disciplines, such as biomechanical engineering, orthopedics, physical medicine and rehabilitation, kinesiology, physical therapy, and sports medicine.

Gait analysis provides a quantitative measure of ambulatory activity. It is used to systematically assess joint kinematics and kinetics, dynamic electromyographic activity, and energy cost/consumption. Methods range from simple visual observation to video recordings and more sophisticated automated computer-based three-dimensional photogrammetric methods. Clinically, gait analysis has demonstrated effectiveness in pretreatment evaluation, surgical decision making, postoperative follow-up, and management of both adult and pediatric patients. It is also used as a tool to enhance elite athletic performance. Within the field of pediatric orthopedics, gait analysis has aided in advancing surgical treatment from single, isolated procedures to more comprehensive multilevel surgeries (1). These procedures include rectus femoris transfers and releases, hamstring lengthenings, tendoachilles lengthenings, gastrocnemius fascia lengthenings, osteotomies, and selective dorsal rhizotomies (2). Gait analysis has also proven useful in understanding more about orthopedic and neuromuscular disorders such as cerebral palsy, myelomeningocele, degenerative joint disease, multiple sclerosis, muscular dystrophy, rheumatoid arthritis, stroke, Parkinson disease, and poliomyelitis (1,2,3,4,5,6). Further applications include assessment of prosthetic joint replacement (7,8,9,10,11,12,13), analysis of athletic injuries (14,15), studies of amputation (16,17,18,19) and orthotic application (20,21,22), and the use of assistive devices (23). Additionally, gait analysis has been used in the evaluation of pharmacological treatment. Examples include botulinum toxin type-A (BOTOX manufactured by Allegran, Inc.), tetanus neurotoxin (*TeNT*), diazepam, baclofen, 45% ethanol, and phenol (24,25,26,27,28,29,30).

Evolution of Human Motion Analysis

The study of locomotion is an ancient endeavor. Early documentation was demonstrated in the practice of Kung Fu by the Taoist priests in 1000 B.C. (31). An interest in locomotion was also manifested in the days of the ancient Greeks. Hippocrates (460 to 377 B.C.), in his work entitled, *On Articulations,* revealed interest in the relationship between motion and muscle function (31). Later, Aristotle (384 to 322 B.C.) investigated animal movement, which was depicted in his work *Animal Spirits* (32). Through a series of observations, Aristotle developed intuitive theories about the control of movement (33). It is believed that his grandson Erasistratus (310 to 250 B.C.), who was an anatomist and physician, was the first to discover the contractile property of muscle (32). Later, the Roman Empire witnessed the birth of the anatomical period. This era is attributed to the Greek physician Galen (131 to 210 A.D.), who worked for the Roman Emperor Marcus Aurelius (32). Galen

classified exercise movement according to a paradigm that utilized the body segment, activity level, motion duration, and motion frequency (31).

Thereafter progress remained marginal until the early seventeenth century with the foundation of modern motion principles by the Italian mathematician Galileo Galilei (1564 to 1642). Galileo described the time and distance parameters associated with moving objects (33). His work was later enhanced by that of the Italian mathematician, Giovanni Alfonso Borelli (1608 to 1679) (32,33). Borelli was the first to introduce mathematical principles to the study of motion, which was previously based on empirical observation. Borelli gave consideration to the motor force, the point of body support, and the resistance to be overcome (32). During the same period, René Descartes (1596 to 1650), a French mathematician, scientist, and philosopher, described the human body as a machine (33). His ideas were considered revolutionary in modern physiology. Both Borelli and Descartes theorized that all physiological processes obeyed the laws of physics (33). Sir Isaac Newton (1642 to 1727), quantitatively augmented the work of Galileo by introducing the concepts of dynamics, mass, momentum, force, and inertia (33). In 1687, Newton authored *Principa,* a publication in which he delineated the principles of dynamics using the three laws of motion and proposed the theory of universal gravitation (33). Paul J. Berthez (1734 to 1806) proposed a correlation between body force and muscle function (32). Around 1820, Chabrier demonstrated the relationship in muscle function between the free and fixed lower extremities (32). These contributions, while remarkable, remained purely observational.

A new era in gait analysis emerged in 1836 in Leipzig with the work of the Weber brothers, Wilhelm and Eduard. With a combined background in physics, mathematics, anatomy, and physiology, the Weber brothers introduced the scientific foundations of the mechanics of human gait (32,33,34). Through a series of experiments, they formulated a mathematical model of the mechanics of human locomotion (32,33). They measured and reported on stance and swing phase, trunk movement, step duration, and step length (34). Even though their contribution was eminent, not all of their theories were accepted. The Weber brothers hypothesized that during swing phase, the limb advanced by gravitational force alone and required no muscular activity. Hence, they suggested that the swinging limb acts as a pendulum attached to the hip (32,33). This hypothesis was challenged and ultimately invalidated by Amand Duchenne (1806 to 1875). Duchenne, the Webers' contemporary working in Paris, conducted a series of experiments with human subjects using electrical muscle stimulation (35). Duchenne demonstrated that it was impossible to advance the swinging limb in paralytic patients due to the absence of thigh flexors. Rather, these patients advanced their limbs by circumduction or by hip abduction. Hence, he concluded that circumduction was a compensatory mechanism, which would not be present if gravity alone was responsible for limb advancement (32,33).

The first graphic plots of human gait were obtained at the Collège de France à Paris and published in 1872 by Gaston Carlet (1845 to 1892), a student of French physiologist and professor, Étienne Jules Marey (1830 to 1904) (36). Carlet was greatly influenced by the work of his mentor, who invented a special shoe-mounted measuring device that recorded foot pressure and contact duration during gait. This device consisted of an air compression chamber, constructed in the mid-metatarsal region of the shoe sole, and connected to a portable tambour and kymograph by means of rubber hoses. The tambour was mounted on the head to measure vertical oscillations of the body during gait. The recording cycle was triggered by pressure applied to a hand held squeeze ball and terminated with pressure cessation (37). The recording mechanism developed by Marey is illustrated in Fig. 1. Carlet modified Marey's apparatus by adding a heel and forefoot chamber with a smoked drum mounted on an axis in the center of a 20 m circle. This design allowed extended and more detailed measurements (32,33). Figure 2 illustrates the apparatus used by Carlet for recording gait.

The late 1800s witnessed a revolutionary advance in motion analysis along with the foundations of modern cinematography. This success is primarily attributed to the creative work of two pioneers, Étienne Jules Marey (38) and Eadweard Muybridge (1830 to 1904) (39,40). Between 1872 and 1887 Muybridge conducted several photographic studies of human and animal locomotion. Figure 3 depicts one of Muybridge's plates, which is a sequence of photographs of a walking child in the sagittal and coronal planes exposed simultaneously. In one of his early studies, Muybridge set up a network of wires across a horse track, and connected them to the shutters

Fig. 1. The recording mechanism developed by É. J. Marey to study human locomotion. From Marey (37).

of a linear array of still cameras. The running horse triggered the wires and sequentially exposed a series of still snapshots (33). In 1879, Muybridge invented the zoopraxiscope, a projector that reconstructed moving images from still photographs (41). The work of Muybridge was an inspiration to Marey, who recognized the importance of motion pictures in his studies of human walking. This realization led Marey to the invention of the chronophotograph, which was reported in 1885 (38). Marey also built a photographic "gun" to capture multiple images of a walking subject at adjustable intervals (33,34). Later, Marey refined his technique and used a black body suit with white reflective stripes to outline the body segments and obtain stick diagrams (33,34).

In 1881, Karl Von Vierordt (1818 to 1884), a German physician and professor of medicine, contributed to the study of human kinematics by analyzing footprint patterns with colored fluid projections. This allowed a description of body segment movement in space during gait (34). In 1895, Wilhelm Braune and his apprentice, Otto Fischer, constructed a mathematical model of human gait consisting of 12 segments. They utilized cadaveric studies to determine anthropometric parameters, which included the center of gravity of each link segment and that of the total body. The model was capable of depicting displacements, velocities, accelerations, and forces during human gait (33,34,42). Braune and Fischer applied the methods of stereometry to the study of human motion. This novel methodology allowed tracking of the instantaneous location of a moving point in three-dimensional space. Consequently, they were able to obtain more accurate and precise calculations of kinematic parameters than those obtained from the two-dimensional photographs of their predecessors. Four cameras were utilized to capture the image of the moving subject. The coordinates were manually digitized

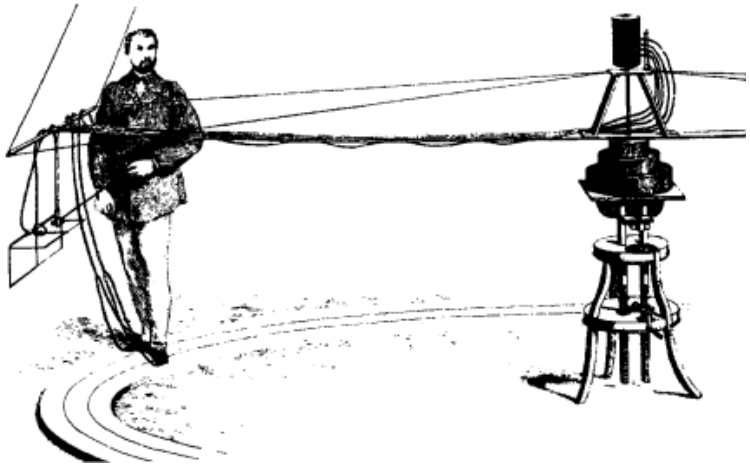

Fig. 2. The apparatus used by G. Carlet for recording gait. Reproduced with permission, from Schwartz and Heath (32).

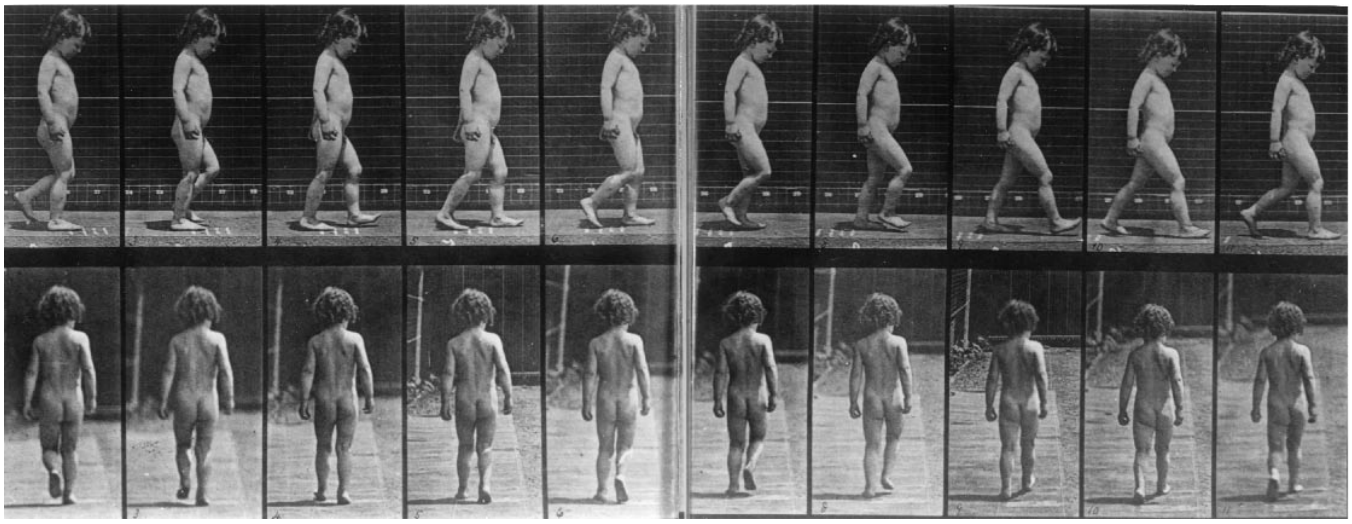

Fig. 3. A sequence of photographs of a walking child. From one of Muybridge's plates (40).

with the aid of a specially fabricated drafting table. In the experimental setup, Braune and Fischer utilized Geisler tubes mounted on a black jersey suit to outline body segments in a manner similar to that used by Marey. Each Geisler tube was filled with rarefied nitrogen and illuminated by an electrical current. Tubes were placed at the head, shoulders, wrists, hips, knees, and ankles. The joint center of each limb segment was identified by the end of the tube corresponding to that segment (33,42,43). Although it took from 6 h to 8 h to prepare a subject for the trial and several months to complete the analysis, the work of Braune and Fischer has been considered as a classical contribution (33,43).

It was not until the twentieth century that a new approach to the analysis of human motion was introduced by Richard Scherb, Chief Surgeon at the Orthopaedic Institute Balgrist in Zürich, Switzerland. Scherb described the pattern and sequence of muscle action of the lower extremities during gait (43). In 1927, Scherb introduced a myokinesiographic method of recording muscle action during locomotion (33). In his early studies,

he utilized palpatory techniques to examine the onset and duration of muscle contractions in individuals walking on a treadmill (33,43). Scherb studied individuals demonstrating gait pathologies including poliomyelitis, spastic paralysis, and hemiplegia (43). In the same year, R. Plato Schwartz introduced the basograph, which was a new apparatus producing graphic records of plantar pressures in normal and pathological gait (44). Subsequently, Schwartz's work underwent a series of refinements. In 1932 he utilized the pneumographic method of Carlet to determine alterations in plantar pressures during gait (32). Schwartz designed a pneumatic shoe to record the plantar pressures. The shoe consisted of three air compression chambers placed under the heel, fifth metatarsal head, and first toe. He was capable of obtaining continuous records of gait parameters by constructing a unique recording mechanism, consisting of pens made from acetate film and special capillary tubes. The experiments were conducted on a concrete floor and on a treadmill. During walking, the soles of the feet were outlined on a plate of ground glass via the use of a transillumination box, thus revealing the respective pressure points. Schwartz utilized a 16 mm motion camera to analyze his records.

The period that followed World War II witnessed exceptional advances in the field of human motion analysis. During this period, the focus shifted toward the dynamic aspects of human gait. Vast contributions are attributed to Inman (1905 to 1980) at the University of California School of Medicine, San Francisco. In 1945, Inman joined Eberhart and Saunders in an extensive study of human locomotion. This project was a collaborative effort between the College of Engineering and the Medical School at the University of California at Berkeley. The work was designed to obtain quantitative data on normal human gait and that of amputees (45).

The multidisciplinary nature of the project required the utilization of several different methodologies (33,43,45,46). A specially designed glass walkway, approximately 10 m long, was constructed for the study. Simultaneous exposure of displacements in the three anatomic planes was done by mounting mirrors beneath the glass surface. Velocities and accelerations of selected points were calculated with excellent precision from the displacement versus time measurements using graphonumerical differentiation. Sagittal displacements were acquired with interrupted light photography, following a similar technique to that designed by Marey. Transverse plane rotations of the lower extremities were obtained with a high degree of accuracy by surgically inserting pins at right angles into the bones of individuals. The degree of rotation at the pelvis, femur, and tibia were determined by measuring the relative displacements of the pins. Electromyographic techniques were also utilized to determine precisely the onset and cessation of dynamic activity of different muscle groups during the gait cycle. Additionally, a force plate dynamometer was utilized to determine the ground reactions: vertical force, torque, horizontal shear, and center of pressure (*COP*) on the foot. Other techniques were subsequently developed to determine the center of gravity locus, relative segment masses, and mass moments of inertia. Rotation measurements between the leg and foot required additional studies of cadaveric specimens. Results from this work were published in 1953 (46).

In 1964, Murray (1925 to 1984) reported on a simple, economical, and repeatable method of recording gait (47). The purpose of this study was to obtain a database with baseline values for normal gait with which pathological gait could be compared. The work was completed in Milwaukee and was a result of a collaborative effort of the Wood Veterans Administration Hospital, the Marquette University School of Medicine, and the College of Engineering at Marquette University.

The study resulted in the depiction of several kinematic gait parameters in the sagittal, coronal, and transverse planes. The parameters included the walking cycle duration and phases: stance phase, swing phase, and period of double limb support; step and stride lengths and widths; foot progression angles; sagittal rotation of the pelvis, hip, knee, and ankle; the vertical, lateral, and forward trajectories of the head and neck; the transverse rotation of the trunk and pelvis; and the sagittal excursions of the upper extremities. Sixty normal male subjects, separated into several categories based on age and height, participated in this study.

The study employed interrupted-light photography in a low-light environment to capture the displacement patterns during gait. Subjects wore reflective fabric over selected anatomical segments and ambulated in front of a Speed Graphic camera with an open shutter. Markers were illuminated via an Ascor Speedlight stroboscope,

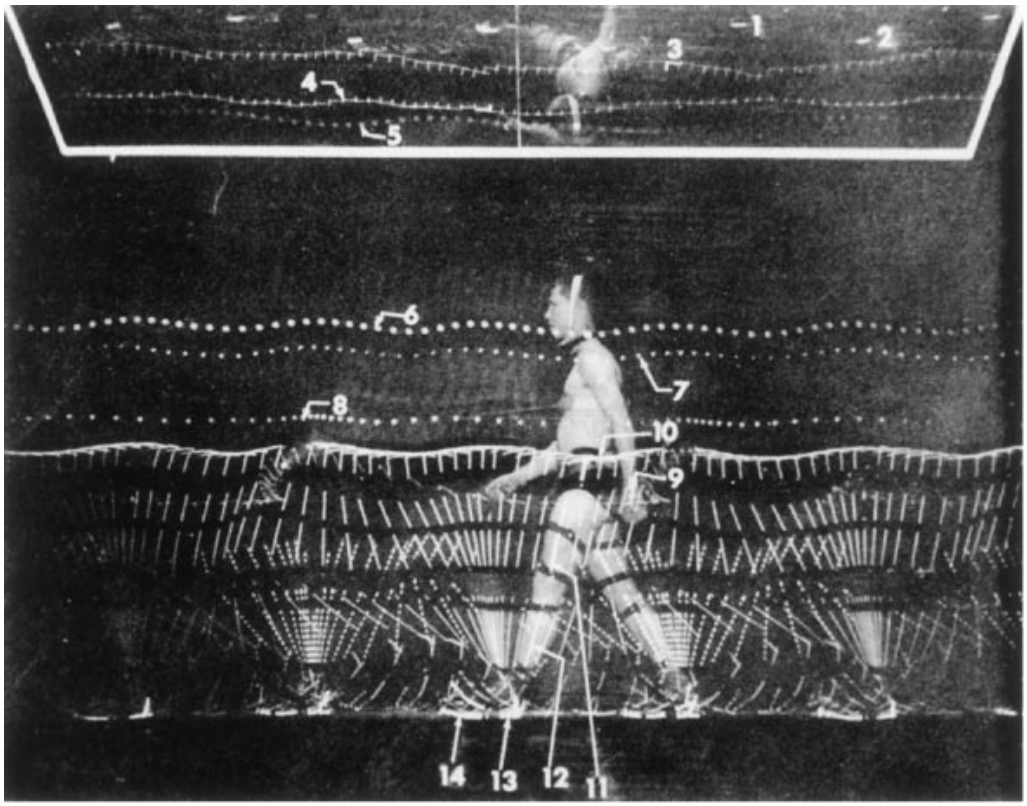

Fig. 4. Interrupted light photography. A typical photograph of a walking subject demonstrated by Murray in a study of human gait. Reproduced with permission, from Murray, Drought, and Kory (47).

flashing at a rate of 20 Hz. Additionally, an Ultrablitz flash unit was fired a single time during the walking trial, which allowed the identification of each marker position on the subject. The resultant photographs depicted a series of stick figures on a black background corresponding to the displacement of the reflective fabric with time. A mirror was mounted over the walkway to simultaneously capture transverse and sagittal plane images. Figure 4 depicts a typical photograph of a walking subject during one of the study trials.

In 1972, Sutherland and Hagy presented a new method for the measurement of gait movements using motion picture technology (48). The novel method employed three 16-mm motion picture cameras positioned at the sides and the front of a walkway in an orthogonal fashion. Marked lines were placed at 30 cm intervals on the long axis of the walkway to provide distance and calibration references for the cameras. During subject testing, markers were placed over bony prominences of the anterior superior iliac spines, greater trochanters, knee joints, ankle joints, and dorsum of the feet between the second and third metatarsal heads.

Following subject testing, the processed film was examined frame by frame on a Vanguard Motion Analyzer (Vanguard Instrument Corporation, New York). The projector featured a tilt control of the image, and a gear to control the X and Y coordinates with dial readout in thousandths of an inch. The film images of the walking subject were projected on a viewer, over which a digitizing grid was superimposed. Measurements were made directly from the projected images, and basic trigonometric functions were used to determine angular displacements. These measurements included transverse plane rotations of the pelvis, femur, and foot and sagittal plane rotation of the knee and ankle. The methods offered several advantages over those used

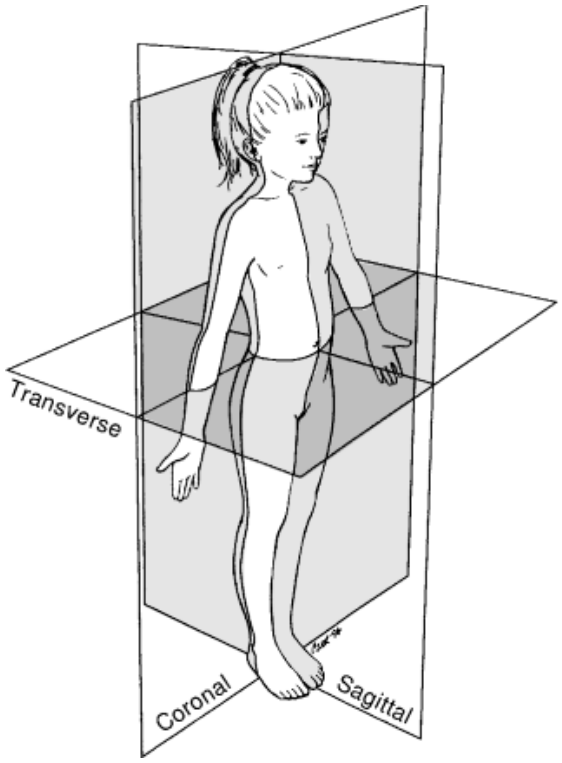

Fig. 5. The human body in the standard anatomical position and the three anatomical planes: sagittal, coronal and transverse.

previously. Subjects were not encumbered with an apparatus and data were recorded during a single session. The method was painless and did not cause discomfort. In addition, electromyograms could be recorded and superimposed onto the motion picture film. This technique also allowed simultaneous bilateral recording. The disadvantages included high equipment cost, and the amount of time required for analysis.

Over the last few decades, increasingly accurate methods of studying human motion have evolved with more widespread clinical applications. Many contributors from various disciplines are responsible for these contributions. Continuous developments in the fields of microelectronics, instrumentation, and bioengineering have advanced the accuracy, reliability, and ease of use of current systems. Today, routine three-dimensional analysis includes joint angles, angular velocities, angular accelerations (kinematic analysis); ground reaction forces, joint forces, moments, and powers (kinetic analysis); and dynamic electromyographic activity (*EMG* analysis). Energy expenditure is also monitored during ambulatory testing in some laboratories.

Anatomic Terminology

This section provides a narrative description of standard anatomic terminology and motion analysis parameters (49,50,51,52,53,54). Human locomotion is defined in all three anatomical planes: the sagittal, coronal, and transverse. These planes are commonly referenced to the human body in the standard anatomical position as depicted in Fig. 5. In this anatomic position, the individual is standing erect with the head facing forward, arms held at the sides, heels joined together, and the feet directed forward so that the great toes make contact.

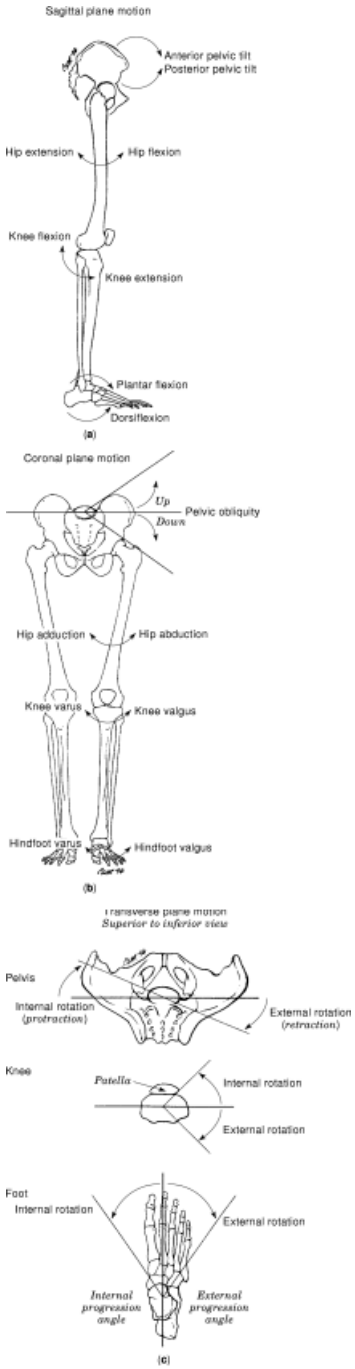

Fig. 6. The types of motion in the three anatomical planes: (a) sagittal plane motion: pelvic tilt (anterior/posterior), hip flexion/extension, knee flexion/extension and ankle plantar flexion/dorsiflexion; (b) coronal plane motion: pelvic obliquity (up/down), hip abduction/adduction, knee valgus/varus and hindfoot valgus/varus; (c) transverse plane motions viewed from top: pelvic internal/external rotation, knee internal/external rotation, foot internal/external rotation and foot internal/external progression angle.

The sagittal plane is a vertical plane that separates the body or body segment into right and left sides. If the sagittal plane divides the human body exactly into left and right halves, then it is termed midsagittal plane. The midsagittal plane is also known as the median plane. The coronal (frontal) plane is defined as the vertical plane that separates the body or body segment into anterior (ventral) and posterior (dorsal) parts. Defined differently, the coronal plane is any vertical plane orthogonal to the sagittal plane. The transverse plane is a horizontal plane that separates the body or body segment into superior and inferior parts. In other words, the transverse plane is any plane orthogonal to both the sagittal and coronal planes.

Directional expressions are used to describe the positions of the body or body segments in the three anatomical planes. The most commonly used directional expressions are anterior, posterior, superior, inferior, medial, lateral, proximal, and distal.

Anterior (ventral) is the direction pointing toward the front of the body or body segment. Posterior (dorsal) is the direction pointing toward the back of the body or body segment.

Superior (cephalic) is the direction pointing toward the head. Superior also denotes the upper part of a structure. Inferior (caudal) is the direction pointing away from the head toward the toes. It also refers to the bottom part of a structure. Medial is the direction that points toward the midsagittal plane of the body or midline of a structure. Lateral is the direction pointing away from the midsagittal plane of the body or midline of a structure. Proximal is the direction closer to the attachment of an extremity or limb to the trunk. Distal is the direction farther away from the attachment of an extremity or limb.

Motion analysis requires that the movements of the body or body segments in the three anatomical planes be accurately described. Figure 6 illustrates the types of motion in the three anatomical planes: (a) sagittal plane motion; (b) coronal plane motion; and (c) transverse plane motion. Sagittal plane motion is often characterized by the terms flexion and extension. Flexion is described as the action that decreases the angle formed between two articulating bones, whereas extension is described as the action that increases the angle. Plantarflexion and dorsiflexion are expressions associated with foot and ankle motion. Plantarflexion is described as the excursion of the foot in the sagittal plane away from the anterior tibia. Dorsiflexion is the excursion of the foot in the sagittal plane toward the anterior tibia.

The terms abduction, adduction, valgus, varus, inversion, and eversion are often associated with coronal plane motion. Abduction is defined as the action of moving a body segment away from the long axis, or midline, of the body in the coronal plane. Adduction is described as the motion of bringing the body segment back toward the midline of the body. Valgus is defined as the lateral angulation posture of the distal segment of a joint, whereas varus is defined as the medial angulation posture of the distal segment of a joint. Inversion and eversion are terms related to foot and ankle motion in the coronal plane. Inversion of the foot refers to the sole of the foot turning toward the midsagittal plane of the body, whereas eversion of the foot is the opposite motion.

Motion in the transverse plane is typically restricted to joint rotations and foot progression angles. It is described in terms of internal and external directions. Using the right hand rule for right side joint rotations, if the fingers are curled in the direction of rotation, then internal rotation causes the thumb to point proximally. On the other hand, external rotation is the opposite gesture, causing the thumb to point distally. For left side joint rotations, the left hand rule is used.

Additional terminology used in human motion analysis includes the center of mass (*COM*), center of gravity (*COG*), and center of pressure (*COP*) locations. These terms are often associated with force and moment measurements. The COM is an anatomical point used to locate the body segment mass in a global (three-dimensional) reference coordinate system. The weighted average of the COM of each body segment represents the total body COM. The vertical projection of the COM on the ground is termed the center of gravity (COG). The center of pressure (COP) is the position of the vertical ground reaction force vector, and is the weighted average of all pressures acting on the plantar surface of the foot in contact with the ground. When one foot is in contact with the ground the resultant COP lies within that foot. When both feet are in contact with the ground, the resultant COP lies somewhere between the two feet. However, the exact location depends on the weight distribution between the two feet (55).

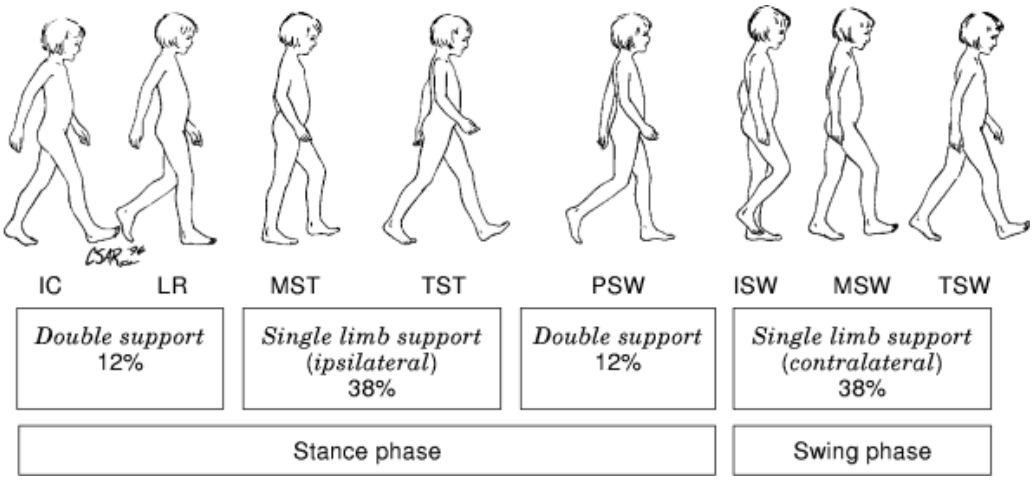

Fig. 7. The gait cycle and its eight events: initial contact (IC), loading response (LR), midstance (MST), terminal stance (TST), preswing (PSW), initial swing (ISW), midswing (MSW) and terminal swing (TSW).

The Cyclic Nature of Gait

Human gait is a cyclic activity that can be described as a series of discrete events. The gait cycle is often defined as the period between initial contact of one foot with the ground and subsequent contact of the same foot (Fig. 7). The gait cycle consists of two major phases: stance phase and swing phase. Stance phase is that portion of the gait cycle when the foot is in contact with the ground, and typically represents approximately 62% of the total normal adult walking gait cycle (49,56,57). Three foot rockers (heel, ankle, and forefoot) occurring during stance phase, serve to control the forward fall of the body during normal ambulation. However, in pathological gait one or more of these rockers may not be present. Swing phase is defined as the period when the foot no longer contacts the ground and the limb advances in preparation for subsequent foot contact (49). Swing phase occupies the remaining 38% of the gait cycle.

The gait cycle is also characterized by eight distinct events, which delineate in an orderly manner specific biomechanical functions (Fig. 7). Stance phase consists of five events: initial contact (*IC*), loading response (*LR*), midstance (*MST*), terminal stance (*TST*), and preswing (*PSW*). Swing phase, on the other hand, consists of the other three events: initial swing (ISW), midswing (*MSW*), and terminal swing (*TSW*) (56).

Initial contact occurs when the foot strikes the ground and marks the beginning of stance phase. In normal walking, initial contact is often referred to as heel strike. For individuals with pathology, heel contact may not occur, hence the term IC is more appropriately used. During IC, the body COM is at its lowest position and the leg is positioned to begin stance with the heel rocker, also termed first foot rocker [Fig. 8(a)] (57,58). The heel rocker occurs as the heel contacts the ground at IC and progresses until the foot plantar flexes into full ground contact (foot flat). At IC, foot contact is made at a single point, causing the heel rocker to behave as an unstable lever system. Consequently, the foot is forced to pivot forward during the period of loading response (LR) with the fulcrum at the heel. During the heel rocker the pretibial muscles (tibialis anterior, extensor digitorum longus, extensor hallucis longus, peroneus tertius) undergo controlled eccentric (lengthening) contraction to resist the external moment created by gravity. This eccentric contraction causes the heel rocker to act as a shock absorber, which decelerates the foot at IC (57,58).

Loading response is the first period of double limb support defined from IC (0%) to approximately 12% of the gait cycle (56,57). During this period, the limb acts as a shock absorber resulting in knee flexion, coincident

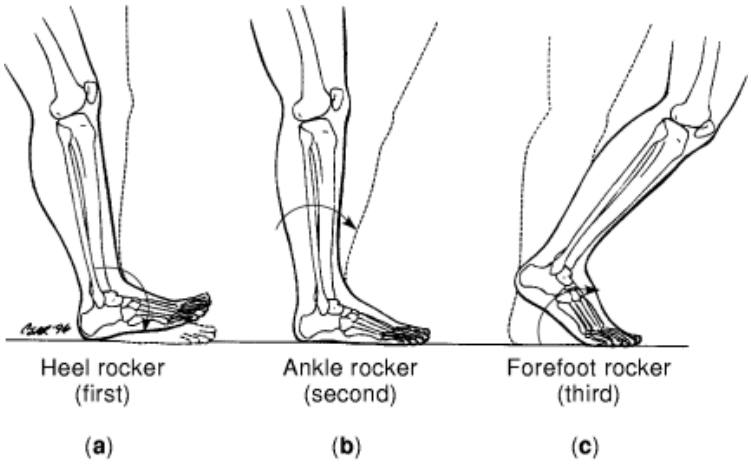

Fig. 8. The three foot rockers occurring during stance phase of the gait cycle: (a) the heel (first) rocker; (b) the ankle (second) rocker; (c) the forefoot (third) rocker.

with load acceptance and deceleration of the body. The period from IC through LR is termed weight acceptance. It is during weight acceptance that the leg provides weight-bearing stability, shock absorption, and control of forward progression (50,56,57).

Single limb support marks the period from midstance (MST) through terminal stance (TST). During this period the opposite (contralateral) limb is in swing phase. Since normal walking is symmetrical this period occupies 38% of the total gait cycle. Midstance (MST) is the period immediately following the loading response (LR). It covers the first half of single limb support from approximately 12% to 31% of the overall gait cycle (50,56,57). Midstance begins when the contralateral foot clears the ground, initiating opposite limb swing phase, and ends at the instant when the body COM is decelerating as it passes over the stance limb forefoot. Midstance is the period of the ankle rocker (second foot rocker), when the ankle dorsiflexes [Fig. 8(b)] (57,58). Momentum forces the tibia to rotate forward over the plantigrade foot with the fulcrum at the ankle (57,58). The ankle rocker begins with foot flat and ends when muscle action restrains further dorsiflexion. This is caused by eccentric contraction of the plantar flexor muscles (gastrocnemius and soleus), primarily the soleus (57).

Terminal stance (TST) comprises the second half of single limb support, which covers from 31% to 50% of the overall gait cycle (50,56,57). This event begins at the time of heel rise and extends until the contralateral limb contacts the ground (opposite foot contact). During this period, the body COM leads the forefoot and accelerates as it is falling forward toward the unsupported limb. Terminal stance is the period of the forefoot rocker (third foot rocker) [Fig. 8(c)] (57,58). This rocker begins at the end of MST and early TST as the body center of pressure (COP) approaches the metatarsal heads and the heel starts to rise. During this period, the metatarsophalangeal joints simulate a pivoted hinge, which functions as a rocker for the forward fall (57,58). This forward fall is initiated as the body COM leads the COP. During this period, the plantar flexors undergo concentric (shortening) contraction. This causes the forefoot rocker (third rocker) to serve as an acceleration rocker to prepare for limb advancement in PSW.

Preswing concludes stance phase. It is also the final period of double limb support, which extends from 50% to 62% of the overall gait cycle (56). Preswing begins at IC of the contralateral limb and ends at terminal contact of the ipsilateral (stance) limb, just as the stance foot clears the ground (50,56,57). This period concludes stance phase and marks the beginning of swing phase. In normal gait, the hallux (great toe) is often the last

foot segment to clear the ground prior to swing. This final stance phase event is also termed "toe off." For individuals with pathology, toe off may not occur, hence "foot off" becomes a more suitable term.

Swing phase constitutes the last phase of the gait cycle, and is associated with limb advancement (56). During this phase, the swinging leg acts as a compound pendulum (56,59,60). The period of the pendulum is controlled by the mass moment of inertia. Variations in gait cadence are highly dependant on an individual's ability to alter the period of this pendulum. Initial swing is initiated at toe off and progresses to the instant where the swinging limb is aligned with the contralateral limb. It is a period of modulated acceleration covering the time from 62% to 75% of the overall gait cycle and usually occupies one third of the swing phase (50,56). Midswing originates when the swinging limb is aligned with the contralateral limb, and is terminated when the swinging limb is in front of the stance limb (and the tibial shaft is vertical). It is a transitional period covering the middle third of swing phase from 75% to 87% of the overall gait cycle (50,56). Terminal swing is initiated with vertical tibial alignment and continues until IC. It constitutes the last third of the swing phase, from 87% to 100% of the overall gait cycle (50,56,57).

Stride and Temporal Gait Parameters

The gait cycle is also characterized by stride and temporal parameters. These consist of step length (meters), step time (seconds), stride length (meters), stride time (seconds), walking speed (meters per second), cadence (steps per minute), single limb support time (seconds), double limb support time (seconds), and stance-to-swing ratio. These time and distance parameters provide an index of an individual's walking patterns. Even though walking is a characteristic activity, there is slight variation in walking pattern from one individual to another. Any deviation in these parameters from normal values will challenge walking efficiency, and hence may affect energy expenditure (57).

Step length is the longitudinal distance from IC of one foot to contralateral IC. Step time is the elapsed time associated with the step length. Stride length is the longitudinal distance between IC of one foot and subsequent ipsilateral IC. Normal gait is symmetrical, hence stride length is equal to twice the step length. Stride time is the elapsed time associated with the stride length. Walking speed is the rate of change of linear displacement along the predefined direction of progression per unit time. Cadence is defined as the rate at which an individual ambulates and is measured in steps per minute. The rate at which an individual ambulates at a self-selected comfortable speed is termed natural cadence. Single limb support is the elapsed time of the gait cycle during which one foot contacts the ground. Double limb support is the elapsed time of the gait cycle during which both feet are in contact with the ground. Single and double limb support may also be expressed as a percentage of the overall gait cycle. Stance-to-swing ratio is the stance interval divided by the swing interval (50,61,62,63). The stride and temporal gait parameters are highly dependant on one's walking speed. Therefore, it is highly recommended that individuals walk at their freely selected cadence during a gait analysis exam.

Although stride and temporal gait parameters are often helpful when diagnosing pathological conditions and evaluating treatment efficacy, they rarely provide sufficient insight into the origin of gait abnormalities (63).

Gait Analysis Methodologies

Gait analysis has advanced a long way since the early days of Marey and Muybridge who utilized the photographic gun and multiple-still camera methods to describe human motion. Currently, several methods are employed in gait analysis to quantify this motion. These approaches include simple visual observation, video

recording, interrupted light photography, cinematography with manual digitization, electrogoniometry, multiaxial accelerometers, and automated three-dimensional motion tracking systems.

Observational Gait Analysis. Observational gait analysis is a useful clinical tool. It is performed by simple visual observation of a walking individual. Although subjective, this method allows a trained examiner to identify many gait deviations during both stance and swing phases. This method is best performed by systematically focusing on one body part at a time. This work is often simplified with the aid of an evaluation form. Observing gait with the naked eye, however, is subject to numerous limitations. In this method, it is difficult to focus concurrently on multiple events and multiple body segments. According to Gage, events that occur faster than 1/16 s (62.5 ms) cannot be visually perceived (63). Hence, gait deviations may be missed even with a trained observer. Furthermore, this method cannot differentiate between primary abnormalities and compensatory responses. To avoid observational misinterpretation, discretion is advised. For example, apparent ankle equinus during initial contact may actually be a neutral ankle with flexed knee. Also, an apparent knee valgus during midstance may actually be a flexed knee and internal hip rotation. In spite of these drawbacks, observational gait analysis remains a useful clinical tool when used with other quantitative measures.

Video Recording. The use of relatively inexpensive electronic equipment can provide refinement to observational gait analysis. A single video camera with a simple monitor (monochromatic color) and a video cassette recorder (*VCR*) yield a functional recording setup. The camera type can be based on a Vidicon tube or a charge-coupled-device (*CCD*) solid state detector. Today, video cassette recorders include advanced features such as freeze-frame, frame-by-frame view, and slow-motion replay. These features allow significant improvement over unaided visual observation. With this method, more consistent observations are obtained when motion videos are reviewed in slow motion rather than reviewing repeated normal speed walks. This method can be further expanded to accommodate simultaneous recording of sagittal and coronal plane motion. This can be simply done by adding a digital screen splitter and one or more cameras. There are varying opinions as to which planes of motion are most accurately analyzed with observational analysis. It is ideal to analyze pathology in the three anatomical planes (sagittal, coronal, and transverse). A limitation to this method is that it does not provide any information regarding dynamic electromyographic (EMG) activity or joint muscle torques, and data are not quantifiable.

Cinematography with Manual Digitization. Motion picture or cine technology can be applied in gait analysis to film real-time events for analysis. This procedure is accurate yet time-consuming. The methods used are similar to those described by Sutherland et al. (48,61). Early investigators used markers mounted over anatomical landmarks and wooden wands affixed to pelvic and tibial belts to facilitate identification of body segment motion (61). Manual digitization of marker locations on a frame-to-frame basis allowed quantitative identification of marker positions in two-dimensional space with respect to the focal plane of the camera. This method can be extrapolated to three-dimensional space. However, the three-dimensional identification of marker positions requires the use of two or more cameras, since each marker must be seen by at least two cameras. Normally, walking is sampled at 50 to 60 frames per second (*fps*). On the other hand, when monitoring high-speed activities, higher sampling rates are needed. In these situations high-speed cameras with sampling rates of 200 fps or higher are used. The major disadvantage of cine with manual digitization is the overwhelming processing time needed for both data digitization and operator training (64).

Interrupted Light Photography. Interrupted light photography is a simple technique that produces multiple images of a moving subject on a single photograph. This approach is similar to that employed by Murray (47). A subject, instrumented with reflective markers over anatomical landmarks, walks in front of a still camera with an open shutter to generate a series of stick figures. Interrupted light is produced by one of two methods. The first consists of a stroboscope firing at a rate of 30 flashes per second. The second method employs a rotating disk mounted in front of the lens and utilizes flood lights for illumination. The disk consists of several equispaced holes and rotates at a constant speed to generate the stroboscopic effect. This technique allows stride and temporal gait measurements directly from the photograph. Although restricted to

two-dimensional analysis, interrupted light photography is simple, inexpensive, and does not encumber the subject (33).

Electrogoniometers. An *electrogoniometer* is a transducer that proportionally converts rotary motion to electrical current. It consists of two rigid links coupled by a potentiometer that measures the interposed angle. In measuring joint angular motion, the rigid links are strapped to a proximal and distal limb segment while the electrical output of the potentiometer marks the joint angle. Electrogoniometers can be applied to either two- or three-dimensional joint motion measurement (65,66). The design of electrogoniometers has been refined, allowing use in extremely difficult situations. Current electrogoniometric systems are more flexible and include designs such as parallelogram structures that allow movement outside the plane of measurement (33). Applications include knee joint motion analysis, where the instant center of rotation is continuously changing and cannot be accurately modeled as a simple hinge. Additionally, modifications to the basic electrogoniometer design have allowed its clinical use with orthotics and prosthetics (67,68). Even though electrogoniometer systems provide simple operation and real-time data measurement, they are difficult to apply, measure only relative joint angles, and can encumber a small individual (69).

Multiaxial Accelerometers. *Accelerometers* are transducers used to measure linear and/or angular accelerations. They can be arranged in either uni- or multiaxial configurations. Displacement and velocity sensors can be used in combination with differentiator circuits to measure acceleration. Direct measurement of acceleration can also be obtained with the use of compact accelerometers. These devices are designed according to Newton's second law and Hooke's law (70). The measured acceleration may then be used to derive velocity and position data through numerical integration techniques. However, appropriate selection of initial conditions should be considered (71). Today, commercially available accelerometers allow the measurement of both linear and angular accelerations with six degrees-of-freedom.

Automated Motion Tracking Systems. The most sophisticated method applied in human motion analysis employs automated tracking systems. These systems utilize two to seven cameras arranged around a calibrated capture volume. The cameras are positioned to cover motion in all three planes: sagittal, coronal, and transverse. The capture volume is a region in the laboratory space where the motion of interest occurs. The dimensions for the capture volume are based on demographic data and stride measurements. These values are obtained from published reports of pediatric and adult gait data. The two-dimensional images acquired from each camera are combined to obtain an instantaneous three-dimensional reconstruction of marker trajectories by using stereophotogrammetric techniques. The trajectories are usually described relative to a fixed laboratory frame system. Standard video technology allows sampling at 50 Hz or 60 Hz. However, some systems offer higher sampling rates for high-speed motion analysis. The sampling frequency in these systems can range from 200 Hz to 2,000 Hz.

Currently, commercially available motion analysis systems provide unique marker and software packages and hardware characteristics. The specific analysis capability of each system relies on both the vendor-supplied hardware and software. Several of these systems offer optional features such as marker data filtering, generation of stick figures, analysis of joint velocities, and determination of joint moments and powers. User-friendly graphics aid in the presentation of the resulting data. Additionally, many of these systems provide user access to data files and establishment of a database.

Marker Sets. Markers are used in conjunction with automated multicamera tracking systems. These markers are mounted over predetermined anatomical landmarks: bony prominences, joint axes, and limb axes. Spherical markers are often used, because they ensure that the centroid location of each marker is independent of the camera view angle. Transverse plane rotations typically use wands to increase measurement accuracy. Two types of markers are currently employed with these systems. The first type is a passive retroreflective marker. This type of marker is made of lightweight spheres covered with 3M 7610 reflective tape (St. Paul, Minnesota). Passive markers do not require power packs, but they do require a source of illumination. The reflected light is then captured by the cameras and digitized by the system. Light is usually supplied by strobes of light-emitting diodes (*LEDs*) arranged in one of two modalities: surrounding each camera lens or placed near

each camera. Flood lights may also be used to provide the source of illumination, but they are not recommended because they create visible distraction. An infrared light source is preferable to minimize subject distraction. In this configuration, cameras are equipped with optical filters, selective of light in the infrared spectrum ($\lambda \simeq 860$ nm) (72). Passive markers are useful in full-body gait analysis. However, in systems that are not fully automated user interaction is frequently required for marker identification.

The second type of marker is an actively illuminated (optoelectric) marker, which is placed on the subject. In these systems, the light-emitting diode markers are pulsed at a predetermined frequency. This marker type allows higher sampling rates (200 Hz to 300 Hz), an increased number of markers per unit area, and frequency-coded data sorting. However, active markers require that the subject carry a power pack or tether, which may create subject distraction and gait alteration.

Accuracy and Reliability of Motion Analysis Systems

Camera Positioning. Although the three-dimensional coordinates of a marker, whether active or passive, can be determined when viewed by two cameras, the realities of gait analysis necessitate that four to seven cameras be utilized. The objective of such a strategy is to obtain complete marker coverage at all times, preventing obstruction of one or more markers in situations such as arm swing and the use of assistive devices. If a marker is not viewed by at least two cameras concurrently, then the position must be estimated. A predictor corrector method is frequently used for marker position estimates. Marker dropout can significantly obscure joint motion data and, when manually supplemented, represents at best an educated estimate of the actual marker position. Such estimates can be deceptive, especially in the analysis of gait patterns (73). The use of multiple cameras increases the overlap and reduces marker dropout. More cameras are necessary to acquire bilateral gait data simultaneously.

Marker Placement. In both active and passive marker systems, the overall accuracy of the system relies on optimal positioning of the markers with respect to anatomic landmarks. A major focus in marker set design is to maximize the distance between markers to reduce image overlap and sorting difficulties. Nonetheless, a resulting drawback is that small body segments such as children's feet cannot always be completely identified or kinematically modeled. Guidelines for marker placement vary widely among systems. Marker placement depends on the biomechanical limb segment model and the procedure for determining joint centers utilized by the system. Common sources of error include inaccurate placement with respect to anatomical landmarks, skin and soft tissue movement, marker dropout from limb swing or assistive device obstruction, trunk rotation, and marker vibration (73,74,75,76). The estimated joint center locations and segment anthropometric data that are based upon markers can be utilized for a preanalysis snapshot, thus increasing the accuracy of characterizing the limb segment geometry with respect to the known marker locations. Figure 9 illustrates a common marker configuration used in lower extremity adult and pediatric gait analysis.

Calibration and Linearization. To reduce potential sources of error, accurate methods of camera linearization and system calibration are required. Linearization is a process used to reduce inaccuracies inherent to camera architecture. These inaccuracies include lens geometry and optical distortion, uncertainty in focal length, aperture setting errors, deviations due to thermal strains, and other nonlinearities inherent in video scanning (77). A two-dimensional linearization grid consisting of a matrix of reflective discs located at precise coordinates is often used in the linearization process. The grid is affixed to a planar surface with proper alignment of the vertical and horizontal axes. The cameras are individually positioned with their focal plane parallel to the linearization grid. The objective is to obtain an image of the grid that covers the entire field of view of the camera. Once this is established, the perpendicular distance between the grid and the focal plane of the camera is measured. Subsequently, data is acquired and a linearization matrix is constructed to correct for errors. This matrix is virtually a one-to-one mapping from the measured target marker coordinates

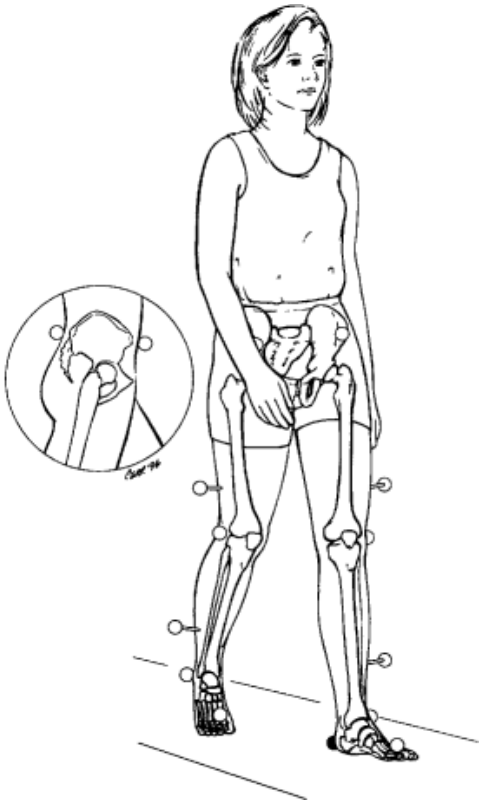

Fig. 9. A common marker configuration used in lower extremity adult and pediatric gait analysis. In this configuration, surface markers are placed over the sacrum at middistance between the posterior superior iliac spines; anterior superior iliac spines; lateral condyles of the knee joint axes; lateral malleoli; and the dorsum of the feet between the first and second metatarsal shafts. Two markers (shown in black) are placed over the posterior heels during static trials only. Marker wands are placed laterally over the lower two-thirds of the femoral and tibial shafts.

to the true target marker coordinates. The linearization procedure should be conducted periodically. However, extensive use of the system requires that linearization be performed more frequently.

Another important attribute in reducing potential errors is system calibration. This is used to correct for variations due to camera placement, temperature fluctuations, and sensor and electronics drift. System calibration is often described in terms of resolution and accuracy. Resolution describes the ability to discriminate position in terms of a linear measure and should be defined with reference to the laboratory capture volume. System accuracy quantifies the maximum absolute difference between a measured variable and its true value. System resolution is usually expressed in terms of millimeters, whereas system accuracy is often described in terms of a percentage of the known separation distance, usually the largest distance in the capture volume. Quantitative characterization of system resolution and accuracy is performed by placing markers at known positions in the capture volume. Measurements outside this capture volume are subjected to extrapolation errors (78). In most gait laboratory facilities, system calibration is routinely conducted on a daily basis. During subject testing both linearization and calibration files are retrieved to perform corrective measures on the kinematic and kinetic data.

Biomechanical Modeling of Gait Data

In human motion analysis the marker set is coupled to a biomechanical or mathematical model that delineates the dynamics of various body segments (14,79,80,81,82). Kinematic data include the instantaneous linear and angular measurements of position, velocity, and acceleration. Measurements may be either absolute or relative. Absolute measurements are referenced with respect to a global (fixed) laboratory coordinate system. Usually, a cartesian coordinate system is selected with the origin located at a specific physical point in the laboratory. Relative measurements are depicted between neighboring body segments and require that the absolute orientation of each segment be obtained first. In three-dimensional motion analysis these relative measurements are commonly known as joint angles. Linear and angular velocities are obtained from the motion data by calculating the change in position per unit time. Typically, this is accomplished on a frame-by-frame basis. The same method is applied for determining accelerations. In most gait analysis laboratories the convention is to describe the motion of the distal segment in relation to the next proximal segment. For example, in lower extremity gait analysis the foot is described with respect to the tibia, the tibia with respect to the thigh, the thigh with respect to the pelvis, and the pelvis with respect to the global laboratory coordinate system. Once the markers are identified in three-dimensional space, their collective position is used to describe the body segment motion characteristics.

Biomechanical models are generally based on the assumption that body segments are rigid bodies. By definition, a rigid body is a system of mass points subject to holonomic constraints such that during motion a constant distance is maintained between all pairs of points (83). A rigid body in three-dimensional space must be represented by a minimum of three noncollinear markers (84,85,86). The spatial relationship among these markers describe the orientation, or attitude, of the rigid body in space. Subsequently, the position and spatial orientation of the rigid body is represented with six degrees-of-freedom or by six independent parameters (2).

Motion that occurs in most anatomical joints is three-dimensional in nature. This motion consists of both translational and rotational components. The rigid body approach can be used in depicting joint motions by looking at the relative position of the proximal and distal body segments about the joint of interest. Each segment is represented by an independent imbedded coordinate system. The motion occurring at the joint is thus described in terms of the relative motion between the two embedded coordinate systems.

To date, several methods have been employed in the description of three-dimensional joint motion. These methods include Euler (Cardan) angles (66,85,87), direction cosines (88), and finite helical (screw) axes (89,90). The Euler and direction cosines methods address only the rotational aspect of joint motion. The finite helical axes method describes the rotation of a rigid body about an axis defined in three-dimensional space, and a translation along that axis. In 1983, Grood and Suntay presented a unique method that utilizes a floating axis (87). Helical parameters have been used by Shiavi to describe knee joint motion (90). Seigler has also used helical parameters to describe motion at the ankle joint (91). The helical axis system, however, is difficult to interpret clinically and may be less useful for describing joint kinematics during gait (85). The Euler system is the most commonly used method clinically for describing three-dimensional motion.

Euler angles describe a set of three successive finite rotations occurring in sequential order about predefined orthogonal (cartesian) coordinate axes. The order of rotations is critical and must be clearly defined. In gait analysis the standard order of rotation is first about the sagittal axis, then about the coronal axis, and finally about the transverse axis. The axis in question being perpendicular to the plane it represents. In this method, a fixed right-handed orthogonal coordinate system is established on each segment and moves with it. The motion of the distal segment is described relative to the next proximal segment. If a three-dimensional unit vector ($\boldsymbol{i}, \boldsymbol{j}, \boldsymbol{k}$) is coupled to the x, y, z axes of the moving segment, and another unit vector ($\boldsymbol{I}, \boldsymbol{J}, \boldsymbol{K}$) is coupled to the X, Y, Z axes of the fixed segment, then the relative orientation between the two segments after any arbitrary finite rotation may be described in terms of three Euler angles (α, β, γ), where α is the rotation about the sagittal axis of the fixed segment, β is the rotation about the line of nodes, and γ is the rotation

about the transverse axis of the moving segment. The line of nodes is a floating axis (coronal axis) orthogonal to both the sagittal axis of the fixed segment and the transverse axis of the moving segment. Each of these angles describes in sequence the rotation of the moving coordinate system with respect to the fixed (reference) coordinate system. In joint motion, the moving coordinate system is within the distal segment and the fixed coordinate system is within the proximal body segment or the laboratory global coordinate system. Figure 10 illustrates the application of Euler angles in describing the relative motion of the femur with respect to the pelvis. The Euler rotational matrix (92) is expressed as:

$$\begin{vmatrix} \boldsymbol{i} \\ \boldsymbol{j} \\ \boldsymbol{k} \end{vmatrix} = \begin{vmatrix} c\beta c\alpha & c\beta c\alpha & -s\beta \\ -c\gamma s\alpha + s\gamma s\beta c\alpha & c\gamma c\alpha + s\gamma s\beta s\alpha & s\gamma c\beta \\ s\alpha s\gamma + c\gamma s\beta c\alpha & -s\gamma c\alpha + c\gamma s\beta s\alpha & c\gamma c\beta \end{vmatrix} \begin{vmatrix} \boldsymbol{I} \\ \boldsymbol{J} \\ \boldsymbol{K} \end{vmatrix}$$

where

c = cosine
s = sine

The fidelity of the biomechanical link segment model used in motion analysis relies on the accuracy of measurements and the reliability of several estimates. The model is coupled to the marker set and is subject to certain underlying assumptions about anthropometric characteristics, such as joint centers, segment length, segment masses, center of mass, and mass moments of inertia. For example, it is assumed that each greater trochanter (hip) marker is at a fixed distance from the center of hip joint rotation. With femoral deformity or hip anteversion this assumption is not accurate. Other sources of errors include any kinematic errors and errors in ground reaction force (*GRF*) measurement. Mathematical techniques used in the biomechanical gait models may also vary somewhat between facilities, thus the kinematic and kinetic data need to be interpreted carefully. This highlights the need for an accurate and thorough clinical assessment with any gait analysis.

Ground Reaction Forces and Plantar Pressures

The ground reaction force (GRF) is an external force acting on the sole of the foot during the activities of standing, walking, or running. This force is a vectorial quantity and, therefore, has both a magnitude and a direction. The GRF is three-dimensional in nature and is usually resolved into a normal (vertical) component and two shear components: anterior-posterior and medial-lateral. Ground reaction forces are commonly measured with force plate dynamometers consisting of strain gage or piezoelectric transducers. In general, force plates are designed to acquired data from six channels, corresponding to the six degrees-of-freedom: $\boldsymbol{F}_x$, $\boldsymbol{F}_y$, $\boldsymbol{F}_z$, $\boldsymbol{M}_x$, $\boldsymbol{M}_y$, and $\boldsymbol{M}_z$; where $\boldsymbol{F}$ denotes the forces along the three global coordinate axes, and $\boldsymbol{M}$ represents the moments about these axes. Force plate data are typically sampled at 600 Hz (100 Hz/channel) and low-pass filtered at 10.5 Hz for quasistatic data and 1050 Hz for dynamic data. A sensitivity–calibration matrix is constructed exclusively for each force platform to convert between raw data (mV) and force (N) and moment (N·m) data.

Processing of force platform output can provide GRF vector components including vertical load, anterior-posterior and medial-lateral shear loads, moments about the vertical axis, and location of the body COP. The vertical load pattern in normal individuals walking at their freely selected cadence follows an M-shaped curve with peak magnitudes of the order of 110% of body weight (80,93). Sutherland et al. reported that children exhibit somewhat diminished average vertical and shear peak forces as compared to adults (93). The vertical load curve is highly sensitive to any gesture that alters the ground reaction vector. For instance, the action of arm lifting can reduce the peak component to less than body weight (94). Additionally, both shear and COP measurements are influenced by the position and movement of all body segments, including the head, arms,

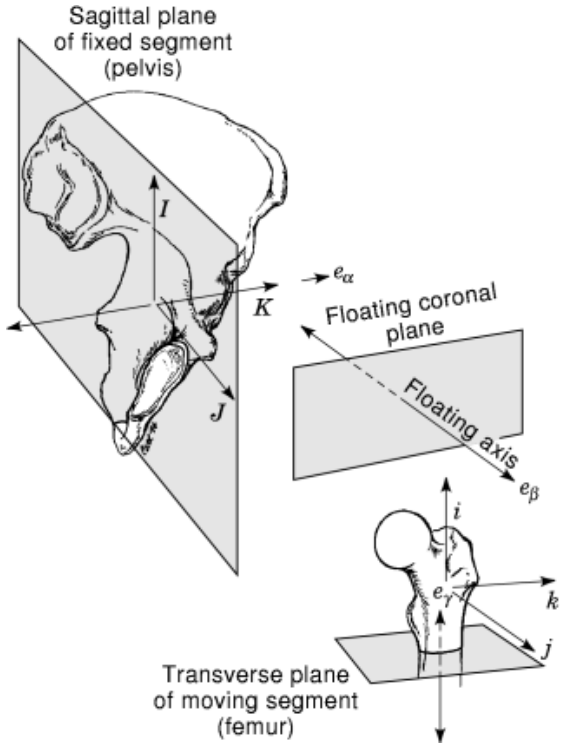

Fig. 10. Euler angle system utilizing the floating axis of Grood and Suntay (87). $\mathbf{e}_\alpha$ is the sagittal axis of the fixed segment (pelvis). $\mathbf{e}_\beta$ is the floating axis (coronal axis) orthogonal to both the sagittal axis of the fixed segment and the transverse axis of the moving segment. $\mathbf{e}_\gamma$ is the transverse axis of the moving segment (femur).

trunk, pelvis, and legs. It has also been reported that disturbances such as pain, weakness, and unilateral hip pathology alter the vertical force pattern (94). Variations in cadence influence the magnitude and duration of the vertical load curve and have a direct effect on the gradient of the M curve, which indicates the rate of limb loading (95,96,97,98).

Pressure measurements under the foot have also been of interest in human motion analysis. To date, numerous measurement techniques have been utilized in the study of the normal and pathological foot. These techniques include floor-mounted transducer matrices, pressure mats, instrumented shoes, insole-based pressure systems, and glass plates using the critical light reflection technique. Alexander et al. provided a recent review of the evolution of current foot-to-ground forces and plantar pressure measurement techniques and their clinical applications (99).

Clinical studies of foot pressures have focused on the anaesthetic foot resulting from diabetes mellitus and Hansen's disease (100,101,102), therapeutic footwear for the insensitive foot (103,104), the planovalgus foot in children with cerebral palsy (105,106), pedorthic inserts for the adult foot (107,108,109), distance running (110), and orthopedic walkers (111).

Studies utilizing floor mounted transducers illustrate barefoot, isolated steps, and insole systems allow investigation of on-going step-to-step alterations in gait for longer durations. It should be noted that in plantar pressure studies consideration should be given to possible sources of error. These include sensor bending, hysteresis, nonlinearities, temperature and humidity changes, and stress shielding secondary to sensor-tissue or sensor-insole interface mechanics (109).

Kinematics

Kinematics is the branch of engineering mechanics in which the motion of bodies is described without consideration of the underlying forces responsible for the movement (57,89). In human motion analysis, kinematics focuses on the study of the relative movement between body segments. These are frequently depicted as rigid link segments. Kinematic parameters include measurements of diarthrodial joint angles, displacements, velocities, and accelerations. In most clinical gait analysis reports, kinematic data are represented in the sagittal, coronal, and transverse planes. In the sagittal plane, joint angular motions include pelvic tilt, hip flexion/extension, knee flexion/extension, and ankle plantar flexion/dorsiflexion. In the coronal plane, joint angular motions consist of pelvic obliquity, hip abduction/adduction, and knee valgus/varus. Transverse plane joint angular motions include pelvic rotation, hip rotation, tibial rotation, foot rotation, and foot progression angle. The patient data are usually presented together with normal control data for comparison. Joint angle depictions may vary with different systems and are highly dependant on the marker arrangement and the biomechanical models employed (50). Furthermore, kinematic data can be supplemented with temporal and stride events that include cadence, walking speed, stride time, stride length, step time, step length, period of single limb support, and period of double limb support. A sample kinematic report is depicted in Fig. 11.

Kinematic data are valuable in the analysis of gait disorders. However, they do not provide information on biomechanical efficiency (oxygen consumption and oxygen cost), ground reaction forces, joint moments, or joint powers. These measurements become important in circumstances where an ambulatory individual presents stable kinematic patterns, but reveals considerable variability in kinetic patterns (112). Furthermore, kinematic gait analysis of an individual with cerebral palsy may not reveal compensatory coping responses (57).

Kinetics

Kinetics is the division of engineering mechanics in which motion is studied with consideration of the underlying forces that cause the movement. These forces include the external ground reaction forces and the internal joint, muscle, and ligamentous forces. The study of human motion analysis is governed by the application of Newton's Second law and Euler's equations of motion (113). The three-dimensional joint reaction forces and moments are obtained from both kinematic analysis and ground reaction forces. At each joint a state of equilibrium exists such that the internal joint reaction forces and moments balance the externally applied forces (114). Moments are often normalized to body weight and leg length, and are expressed as a percent of body weight times leg length (14). Joint powers are calculated once the moments, joint angles, and angular velocities are determined (115). The equations describing joint reaction forces are expressed in terms of Newton's Second law as:

$$\Sigma \boldsymbol{F}_x = m\boldsymbol{a}_x$$
$$\Sigma \boldsymbol{F}_y = m\boldsymbol{a}_y$$
$$\Sigma \boldsymbol{F}_z = m\boldsymbol{a}_z$$

where

$\Sigma \boldsymbol{F}_x$, $\Sigma \boldsymbol{F}_y$, $\Sigma \boldsymbol{F}_z$ = are the sums of external forces acting on a limb segment in the x, y, and z directions, respectively,

m = the mass of the limb segment,

$\boldsymbol{a}_x$, $\boldsymbol{a}_y$, $\boldsymbol{a}_z$ = are the linear accelerations of the center of mass of the limb segment in the x, y, and z directions, respectively.

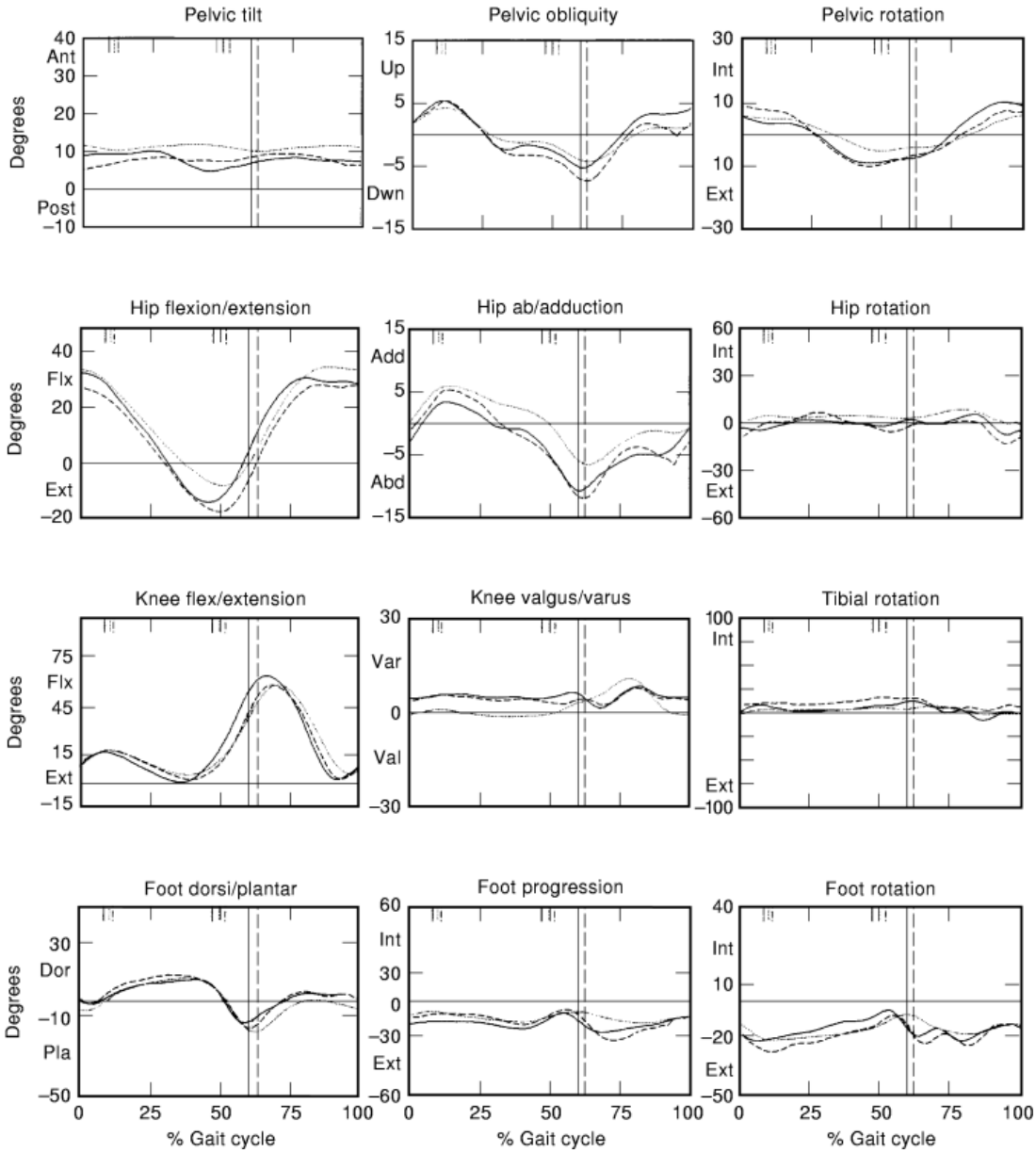

Fig. 11. A sample report of kinematic data in the three anatomical planes. The solid and dashed curves represent the patient's left and right side motions, respectively. The dotted curves represent the mean motion of the laboratory normal sample group. The vertical lines separate stance phase from swing phase. Initial contact occurs at 0% of the gait cycle.

Joint moments are computed using Euler's equations of motion as

$$\Sigma \boldsymbol{M}_x = I_{xx}\boldsymbol{\alpha}_x + (I_{zz} - I_{yy})\boldsymbol{\omega}_y\boldsymbol{\omega}_z$$
$$\Sigma \boldsymbol{M}_y = I_{yy}\boldsymbol{\alpha}_y + (I_{xx} - I_{zz})\boldsymbol{\omega}_z\boldsymbol{\omega}_x$$
$$\Sigma \boldsymbol{M}_z = I_{zz}\boldsymbol{\alpha}_z + (I_{yy} - I_{xx})\boldsymbol{\omega}_x\boldsymbol{\omega}_y$$

where

$\Sigma \boldsymbol{M}_x, \Sigma \boldsymbol{M}_y, \Sigma \boldsymbol{M}_z$ = are the sums of external moments applied to the limb segment in the x, y, and z directions, respectively,

I_{xx}, I_{yy}, I_{zz} = are the mass moments of inertia of the limb segment about the principal axes,

$\alpha_x, \alpha_y, \alpha_z$ = are the angular accelerations of the center of mass of the limb segment in the x, y, and z directions, respectively,

$\omega_x, \omega_y, \omega_z$ = are the angular velocities of the center of mass of the limb segment in the x, y, and z directions, respectively.

Joint powers are calculated as

$$P_x = \boldsymbol{M}_x \cdot \boldsymbol{\omega}_x$$
$$P_y = \boldsymbol{M}_y \cdot \boldsymbol{\omega}_y$$
$$P_z = \boldsymbol{M}_z \cdot \boldsymbol{\omega}_z$$
$$\Sigma P = P_x + P_y + P_z$$

where

P_x, P_y, P_z = are the joint powers in the x, y, and z directions, respectively,

$\boldsymbol{M}_x, \boldsymbol{M}_y, \boldsymbol{M}_z$ = are the external moments applied to the limb segment in the x, y, and z directions, respectively,

$\omega_x, \omega_y, \omega_z$ = are the angular velocities of the center of mass of the limb segment in the x, y, and z directions, respectively,

ΣP = the total joint power.

In most clinical gait analysis reports, kinetic data includes hip, knee, and ankle joint moments and powers. Figure 12 illustrates a sample kinetic report.

Clinically, kinetic analysis has proven useful in examining specific pathological conditions and operative procedures designed to restore normal function. Moment analysis has been useful for clinical decision making in cerebral palsy (116). It has also provided insight into subtle functional adaptations, such as the increased flexion moment observed at the hip and knee in patients with anterior cruciate ligament deficiency (117). Additionally, moment analysis has been recommended for predicting postoperative outcomes of high tibial osteotomy from preoperative knee adductor data (118).

An area of increasing interest and expanding clinical application is that of biomechanical modeling, in which kinematic and kinetic gait data form an integral part of the solution. In contrast to the typical gait analysis solution, in which known motion and body segment parameters are used to estimate internal joint kinetics, these biomechanical models focus on an analysis of muscle function and effects. Typically, the more advanced biomechanical models address the following issues: alteration of muscle moment arm through surgery, alteration of muscle force generation through surgery, estimation of muscle length during normal and pathologic movement, and visualization and physical appreciation of interactions between muscle activity and kinetic gait parameters (119).

Zajac et al. have developed biomechanical models based on detailed physiological considerations, including characteristics defined in the original Hill muscle model (120). Dynamics of contraction are determined by considering muscle output as two independent first-order processes: activation dynamics and contraction dynamics. A generic actuator is developed and scaled to specific muscle and tendon parameters including peak isometric force, optimal muscle fiber length, tendon slack length, and maximum shortening velocity. The model clearly demonstrates that the muscle acts as a central nervous system (*CNS*) controlled force generator, demonstrating a frequency response dependent on actuator length and/or activation level input. The muscle can also act as a spring, dashpot, or combined passive element, again dependent upon CNS control (120).

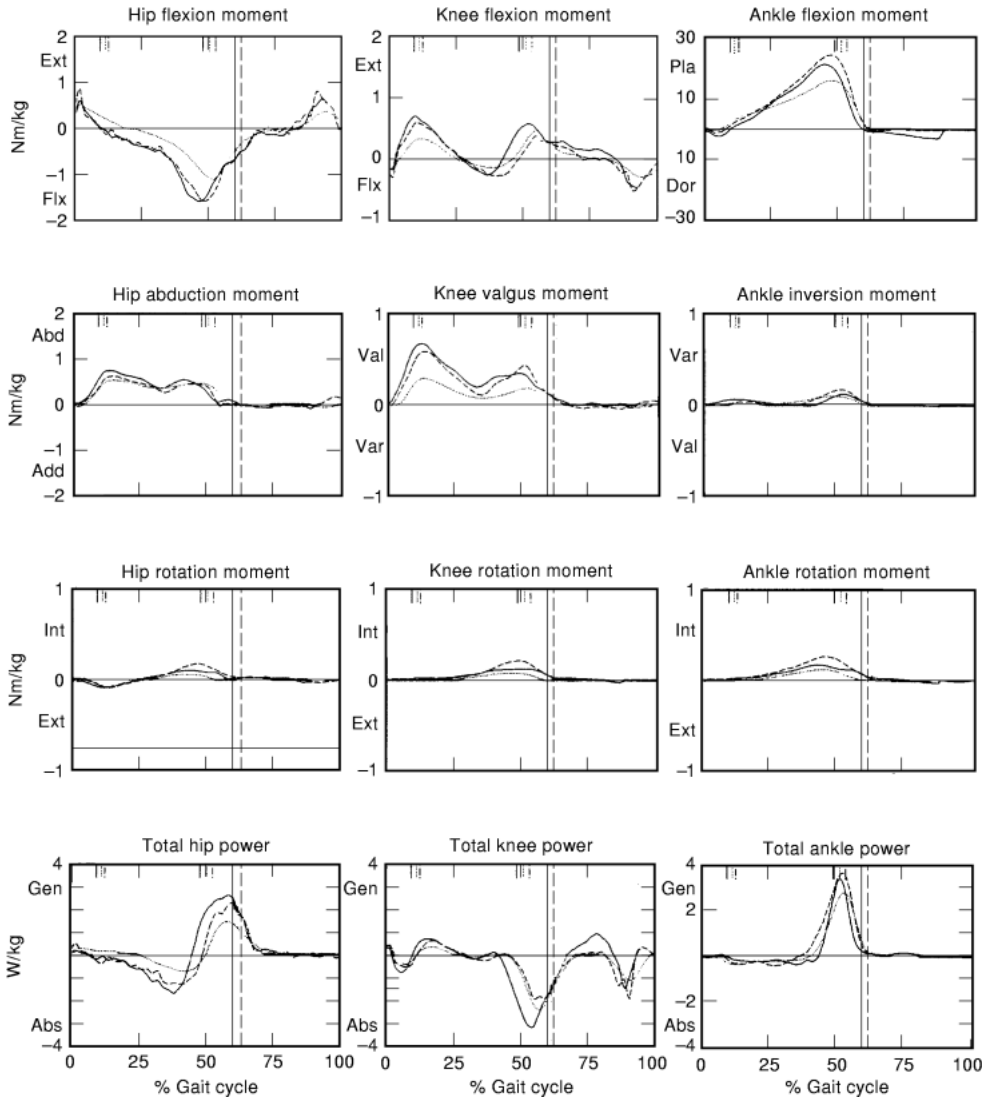

Fig. 12. A sample report of kinetic data in the three anatomical planes. The four rows represent sagittal plane internal joint moments; coronal plane internal joint moments; transverse plane internal joint moments; and total joint powers. The three columns represent: hip, knee, and ankle joint data. The solid and dashed curves represent the patient's left and right side data, respectively. The dotted curves represent the mean results of the laboratory normal sample group. The vertical lines separate stance phase from swing phase. Initial contact occurs at 0% of the gait cycle.

Delp et al. have developed a graphics-based computer model to illustrate the effect of various surgical procedures upon gait kinematics and kinetics (119,121). These models use many of the physiological considerations included in Zajac's models. Using a computer graphics work station, Delp et al. can alter the biomechanical models to study how various surgical procedures, such as osteotomies, tendon transfers, or tendon lengthenings, affect the moment arms and force-generating characteristics of the muscles. The models can also be used in conjunction with gait data to study muscle function during ambulation. Currently, the model represents an adult male with a height of approximately 1.8 m and a mass of 75 kg (119).

Dynamic Electromyography

Dynamic EMG indicates muscle function by recording the voltage potentials generated by the electrochemical activities in the muscle. It provides detailed information about the timing and relative intensity of muscle activity. Nevertheless, dynamic EMG does not tell us about the strength of the muscle, whether the muscle is under voluntary control, or whether the contraction is isometric, concentric, or eccentric (122). The instrumentation needed for accurate recording of the EMG signal consists of recording electrodes, signal amplification and conditioning circuitry, signal transmission, and a means for data display and storage (123). Myoelectric signals can be recorded by three types of electrodes: needle, surface, and fine-wire. Needle electrodes are commonly employed for diagnosis of muscle disorders and are not recommended for gait analysis due to the discomfort they produce.

In gait analysis, both surface and fine-wire electrodes are used for dynamic EMG analysis. Surface electrodes are placed on the skin over targeted muscles. Two types of surface electrodes are frequently used in routine gait analysis: Silver–silver chloride (Ag–AgCl) disks and active electrodes with built-in amplifiers and filters to improve signal quality and reduce noise effects. Silver–silver chloride electrodes consist of both a pickup and a reference disc. These electrodes require that the skin surface be cleansed and a conductive paste gel be used to minimize interface impedance at the recording site. It has been recommended that the Ag–AgCl disks be separated by 1 cm to obtain improved signal quality from the targeted muscle (124). Active electrodes have three terminals: reference, ground, and recording. These electrodes produce better signal quality because of their high input impedance and, hence, do not require epidermal preparation and conductive paste (124). Advantages of both types of surface electrode is that they are noninvasive, easy to apply, reusable, produce repeatable results, and can detect activities of muscle groups. However, disadvantages of both types of surface electrode is the inability to record activities from specific muscles and crosstalk from neighboring muscles. In situations where the monitoring of the activity of specific and deep muscles is required, the use of fine-wire EMG becomes necessary (125,126).

Fine-wire EMG is a technique used to measure myoelectrical activity directly from individual muscles. In this method, a small-gauge hypodermic needle containing a pair of fine wire electrodes (one active, one reference) is inserted into the muscle of interest. The needle is then pulled out, leaving the two fine wires positioned within the muscle. Confirmation of the correct placement of the electrodes within the muscle is then determined by stimulating the muscle electrically through the fine-wire electrodes. Palpation and observation of the target muscle or tendon are used concurrently during the confirmation procedure (123,127). To avoid electric shorting, the electrodes are staggered by a few millimeters at their bared tips (123). The most common type of fine-wire electrode used in dynamic EMG is a nickel–chromium alloy wire (50 μm in diameter) with teflon insulation. The greatest advantage of fine-wire EMG is muscle selectivity. Recordings may be obtained from small peripheral muscles or those deeply located. However, this method is invasive, requires skilled placement, and may require multiple insertions. A new technique was introduced by Park and Harris in 1996 that avoids additional needle insertion. This technique monitors the electrical signal from the muscle while the needle with the fine-wire electrodes is advanced. This signal serves to guide the needle into the proper muscle (127). Muscle crosstalk is also present with fine-wire EMG. However the spectral content of the signal recorded with the fine-wire electrode allows filtering of some of the lower frequency volume conducted signals and thus allows reduction of muscle crosstalk.

Both surface and fine-wire electromyographic signals have small amplitudes and do not allow direct interpretation without amplification. A differential amplifier with high common mode rejection (*CMR*) is used to eliminate electrical noise seen by both electrodes. The myoelectric signals recorded by surface and wire electrodes have different spectral characteristics of known bandwidths. Surface EMG signals have a bandwidth of 10 Hz to 350 Hz, with a mean frequency of 50 Hz. Fine-wire EMG signals have bandwidth of 10 Hz to 1000 Hz, with a mean frequency of 350 Hz. The lower bandwidth observed in surface EMG is a result of attenuation of higher frequencies as they travel through the tissues. The quality of the EMG signal is improved by filtering

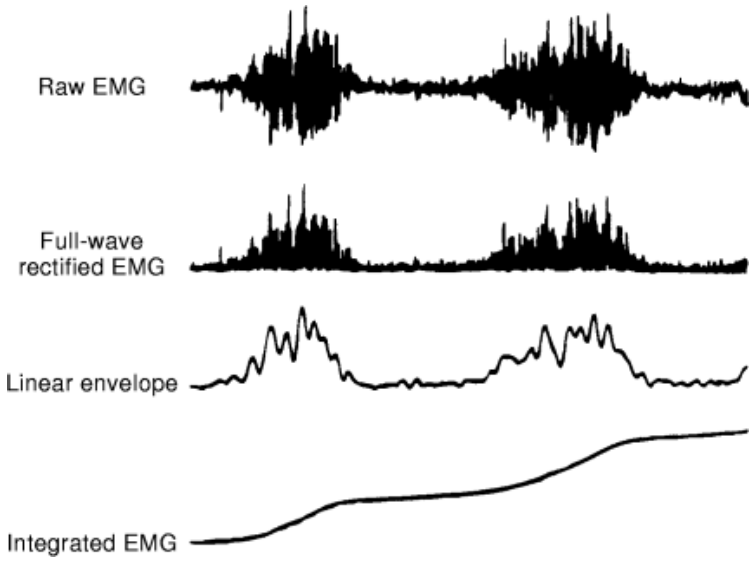

Fig. 13. Dynamic EMG data. The first row represents a typical raw EMG signal recorded with active electrodes; the second row represents a full-wave rectification (absolute value) of the raw EMG signal; the third row represents the result of linear envelope (moving average) of the rectified EMG signal; and the fourth row represents the integrated processing (area under the curve) of the rectified EMG signal.

rejected frequencies. Motion artifacts, introduced by the subject or wires, have a low frequency content of 10 Hz to 20 Hz and can be reduced by increasing the low frequency cutoff.

Commercial electromyographic systems are currently available with either cable or telemetry designs, or a combination of both. Cable systems are more reliable and less expensive than telemetric systems. However, they may encumber the subject with multiple tethers. Telemetric systems are based on radio frequency (RF) and are susceptible to electromagnetic interference. Telemetric systems may also require more frequent technical service. Other commercial systems are based on a combination of cable and telemetry design. These are capable of transmitting multiple signals on a single cable and offer numerous advantages over both systems.

Automated methods for determining the onset and cessation of dynamic EMG have been reported (128). The raw EMG signal can either be analyzed or processed. A higher sampling rate is required to accurately acquire raw EMG signals. The most common methods of EMG signal processing are full wave rectification, linear envelope or moving average, and integration of the full wave rectified EMG (Fig. 13). The linear envelope is created by filtering a full-wave rectified signal with a low pass filter. The linear envelope is useful to assess on and off activity, but clonus bursts of muscle activity may not be seen (122).

Many variables influence the recorded EMG signal such as magnitude of tension, velocity of shortening, rate of tension buildup, fatigue, and reflex activity (81). The relationship between the EMG signal and the force generated has been studied extensively (129,130,131,132,133,134) but needs to be interpreted with extreme caution in gait. Dynamic EMG does not indicate the strength of a muscle or the torque generation about a joint. There can be constant change throughout the gait cycle in multiple factors known to affect the relationship between the EMG signal and the force generated, such as the joint angle, the muscle fiber length, and the type of contraction (concentric, eccentric, or isometric). There is a great deal of interest in the relationship between the EMG signal and muscle force-joint torque. Early theoretical studies by Moore (135) and Libkind (136) suggested that during controlled isometric contraction, the EMG signal amplitude should increase as the square root of the muscle force generated. According to Basmajian and DeLuca, few experimental results

support the square root relationship (137). Muscle activity during gait is far more complex than simple isometric contraction, further complicating any direct relationship between the EMG signal and muscle force or joint torque.

In pathologic gait, dynamic EMG is useful in preoperative evaluation of ankle and hip deformities (138, 139,140) and in analysis of rhizotomy results (141,142). Dynamic EMG in conjunction with kinematic analysis plays an important role in evaluating gait in individuals with neuromuscular disorders. The dynamic EMG signal is analyzed to identify whether the rectus femoris is firing continuously during swing phase. Posterior transfer of the distal rectus femoris has been found useful to augment knee flexion during swing in some individuals (143). Overall indications for rectus femoris transfer include a positive Duncan-Ely test, dynamic EMG evidence of prolonged swing phase rectus femoris activity, and reduction of swing phase knee motion by at least 20% (144,145). Analysis of dynamic EMG timing is also important in evaluating ankle valgus and varus deformities, although there is controversy regarding the role of dynamic EMG in posterior tibialis surgical procedures in cerebral palsy (133,140,146).

Energy Expenditure

Gait requires kinetic energy expenditure as the body segments move, and potential energy generation as ligaments and elastic elements of muscle are stretched and as the COM moves vertically (53,57). Only 50% of potential energy is recovered during gait (147). An important role is played by two joint muscles that transfer energy between proximal and distal segments (148). The six determinants of gait, as described by Saunders, Inman, and Eberhart (46), work to minimize the total excursion of the body center of gravity and thus conserve kinetic energy. The body center of mass is highest during midstance, which is when the horizontal displacement is the least. The horizontal displacement is greatest during double limb support, which occurs when the COM and potential energy are lowest. Analysis of this two-dimensional sinusoidal pattern of displacement of the COM may underestimate the energy expenditure, because it may not properly reflect changes in body segment energy other than that of the trunk (57,149,150).

The energy requirements for ambulation can be assessed during gait analysis. Heart rate data have been described as an index of energy expenditure for normal children and children with cerebral palsy (151). A linear relationship between heart rate and oxygen uptake at submaximal heart rates has been noted during normal gait (152). Information regarding oxygen uptake can be gathered with a modified Douglas bag technique or a mobile gas analysis system on a cart that is pushed alongside the subject during ambulation. Oxygen consumption (mL O_2/kg/min) and oxygen cost (mL O_2/kg/m) can be calculated. Heart rate and oxygen uptake data during ambulation are compared to data gathered during quiet sitting and quiet standing, and to age-matched normals because there is an age-dependent linear relationship between walking velocity and oxygen consumption (153).

Interpretation and Decision Making

The most frequent use of gait analysis is as a quantitative aid in surgical decision making. Other useful information is obtained through careful physical examination. Gait analysis has also proven beneficial in documenting the effects of treatment and to describe the natural progression and history of various neuromuscular conditions.

The interpretation of quantitative gait data requires a multidisciplinary team with expertise in engineering, kinesiology, physical therapy, and medicine. The methods employed involve presentation of data in an understandable form and evaluation of past studies, if available, to define a natural history. In those

individuals with pathology a recommendation for intervention, if appropriate, is based upon available treatment modalities and technology.

Patient data should be presented in a clear and understandable format. This requires a graphic representation of kinematic, kinetic, and EMG data, as well as that of a normal control population. In addition, review of photographs of subject marker placement, and video tapes of walking are helpful in understanding and appreciating the motion patterns. Radiographs are also reviewed at the time of analysis in those cases where musculoskeletal pathology is involved.

Sutherland et al. have described the important effects of growth and maturation on the development of mature walking patterns in normal children, and this process is also known to occur over a longer time span of many years in children with neuromuscular disorders (154). Continued observation with maturation is necessary to track developmental abnormalities over time.

The interpretation of gait analysis requires that deviations from normal be identified. These deviations are then separated into primary abnormalities and secondary compensations. A primary abnormality is defined as deviation from the normal gait pattern caused by contracture or muscle abnormality in an affected joint. Secondary compensations are strategies employed to optimize gait. For example, a person may walk with plantar flexion of the ankle because of a limb length discrepancy and shortening of the affected side. The examination of the patient along with EMG and kinetic data are useful in separating primary abnormalities from secondary compensations.

Clinical recommendations are generally made to improve function. There are many ways to define a normal functioning gait pattern, including temporal and stride characteristics. More specifically, the prerequisites for normal gait can be classified into five areas: (a) stance phase stability; (b) adequate foot clearance; (c) preposition of the foot in swing; (d) adequate stride length; and (e) energy conservation through minimization of the excursion of the COG (57). Focusing on these specific prerequisites can aid the clinician in making treatment recommendations.

The process of gait interpretation and decision making varies among laboratories. Most laboratories document the evaluation with a written report detailing gait abnormalities, and treatment recommendations with reference to any previous studies. The report is generally prepared by a multidisciplinary group, as described above. Most clinical gait laboratories also retain records of patients to comprise a database, which can be referenced for particular individual patients and also to study groups of patients sharing similar pathologies.

Future Trends in Gait Analysis

Current and future directions in gait analysis will include more sophisticated tools for the analysis and interpretation of data such as pattern analysis, neural networks, and artificial intelligence. There is potential for much greater clinical application of moment and power data. Future biomechanical modeling of gait data will routinely include upper body segments and allow analysis of the flow of energy and power between body segments. More sophisticated models will also allow accurate analysis of the biomechanical effects of orthotics, prosthetics, and assistive devices. Because of competition and technological advances, it is expected that gait analysis systems will become less expensive and more accessible for routine clinical applications. Data banks with pretreatment and posttreatment results will need to be established through multicenter clinical studies. Continued mathematical synthesis of gait, anthropometric, and physiological data will improve musculoskeletal computer modeling, which in turn may improve pretreatment assessment, surgical planning, and postoperative followup.

Acknowledgments

The authors would like to extend their appreciation to Mr. Gautam Sampath for his kind assistance in preparing this manuscript. The authors would also like to express their deep sense of gratitude to the Department of Graphic Arts at Shriners Hospital for Children—Chicago and in particular to Ms. Cynthia S. Armstrong Rosa for the art work. Much of the work referred to in this text was supported through the Shriners Hospitals for Children Research Foundation.

BIBLIOGRAPHY

1. P. A. DeLuca Gait analysis in the treatment of the ambulatory child with cerebral palsy, *Clin. Orthopaed.*, **264**: 65–75, 1991.
2. R. B. Davis P. A. DeLuca Clinical gait analysis: Current methods and future directions, in G. F. Harris and P. A. Smith (eds.), *Human Motion Analysis: Current Applications and Future Directions*, Piscataway, NJ: IEEE Press, 1996, pp. 17–42.
3. D. H. Sutherland *Gait analysis in neuromuscular disease*, San Diego Children's Hospital Instructional Course, 1990, pp. 333–341.
4. S. J. Olney *et al.* Work and power in gait of stroke patients, *Arch. Phys. Med. Rehab.*, **72**: 309–314, 1991.
5. R. C. Wagenaar W. J. Beek Hemiplegic gait: A kinematic analysis using walking speed as a basis, *J. Biomech.*, **25**: 1007–1015, 1992.
6. R. B. Davis P. A. DeLuca S. Õunpuu Analysis of gait, in J. D. Bronzino (ed.), *The Biomedical Engineering Handbook*, Boca Raton, FL: CRC Press, and Piscataway, NJ: IEEE Press, 1995, pp. 381–390.
7. M. C. Collopy *et al.* Kinesiologic measurements of functional performance before and after geometric total knee replacement, *Clin. Orthopaed. Rel. Res.*, **126**: 196, 1977.
8. N. Rittman *et al.* Analysis of patterns of knee motion walking for four types of total knee implants, *Clin. Orthopaed. Rel. Res.*, **155**: 111–117, 1981.
9. M. P. Murray *et al.* Kinesiologic measurements of functional performance before and after double compartment marmor knee arthroplasty, *Clin. Orthopaed. Rel. Res.*, **173**: 191–199, 1983.
10. E. Olsson Gait analysis in hip and knee surgery, *Scand. J. Rehab. Med.*, **15S**: 5–53, 1986.
11. A. T. Berman *et al.* Quantitative gait analysis after unilateral or bilateral total knee replacement, *J. Bone Joint Surg.* **69**: 1340–1345, 1987.
12. A. T. Berman *et al.* Quantitative gait analysis after unilateral or bilateral total hip replacement, *Arch. Phys. Med. Rehab.* **72**: 190–194, 1991.
13. A. Wykman E. Olsson Walking ability after total hip replacement, *J. Bone Joint Surg.* **74B**: 53–56, 1992.
14. T. P. Andriacchi R. P. Mikosz Musculoskeletal dynamics, locomotion, and clinical applications, in V. C. Mow and W. C. Hayes (eds.), *Basic Orthopaedic Biomechanics*, New York: Raven Press, 1991, pp. 51–92.
15. R. Jacobs G. Schenau Intermuscular coordination in a sprint pushoff. *J. Biomech.* **25** (9): 953–965, 1992.
16. R. L. Waters *et al.* Energy cost of walking of amputees: The influence of level of amputation, *J. Bone Joint Surg.* **58A**: 42–46, 1976.
17. H. B. Skinner D. J. Effeney Gait analysis in amputees, *Amer. J. Phys. Med.*, **64**: 82–89, 1985.
18. A. Gitter J. M. Czerniecki D. M. DeGroot Biomechanical analysis of the influence of prosthetic feet on below-knee amputee walking, *Amer. J. Phys. Med. Rehab.*, **70**: 142–148, 1991.
19. G. R. Colborne *et al.* Analysis of mechanical and metabolic factors in the gait of congenital below knee amputees: A comparison of SACH and Seattle feet, *Amer. J. Phys. Med. Rehab.* **71**: 272–278, 1992.
20. J. F. Lehmann *et al.* Gait abnormalities in peroneal nerve paralysis and their correction by orthoses: A biomechanical study, *Arch. Phys. Med. Rehab.* **67**: 380–386, 1986.
21. J. F. Lehmann *et al.* Gait abnormalities in hemiplegia: Their correction by an ankle-foot orthosis, *Arch. Phys. Med. Rehab.* **68**: 763–771, 1987.
22. D. S. Brodke *et al.* Effects of ankle-foot orthoses on the gait of children, *J. Pediatr. Orthopaed.*, **9**: 702–708, 1989.

23. C. Montecucco G. Schiavo Mechanism of action of tetanus and botulinum neurotoxins. *Mol. Microbiol.* **13** (1): 1–8, 1994.
24. L. Logan K. Byers-Hinkley C. D. Ciccone Anterior versus posterior walkers: A gait analysis study, *Dev. Med. Child Neurol.* **32**: 1044–1048, 1990.
25. J. F. Mooney III L. A. Koman B. P. Smith Neuromuscular blockade in the management of cerebral palsy, *Adv. Oper. Orthopaed.*, **1**: 337–343, 1993.
26. L. A. Koman *et al.* Management of cerebral palsy with botulinum-A toxin: Preliminary investigation, *J. Pediatr. Orthopaed.* **13**: 489–495, 1993.
27. A. L. Albright A. Cervi J. Singletary Intrathecal baclofen for spasticity in cerebral palsy, *J. Amer. Med. Assoc.*, **265**: 1418–1422, 1991.
28. E. B. Carpenter Role of nerve blocks in the foot and ankle in cerebral palsy: Therapeutic and diagnostic, *Foot Ankle* **4**: 164–166, 1983.
29. E. B. Carpenter D. G. Seitz Intramuscular alcohol as an aid in management of spastic cerebral palsy, *Dev. Med. Child Neurol.* **22**: 497–501, 1980.
30. G. Tardieu *et al.* Treatment of spasticity by injection of dilute alcohol at the motor point or by epidural route. Clinical extension of an experiment on the decerebrate cat, *Dev. Med. Child Neurol.* **10**: 555–568, 1968.
31. J. V. Basmajian *Therapeutic Exercise*, 3rd ed., Baltimore: Williams & Wilkins, 1978, pp. 1, 3, 5.
32. R. P. Schwartz A. L. Heath The pneumographic method of recording gait, *J. Bone Joint Surg.* **14**: 783–794, 1932.
33. M. E. Johanson Gait laboratory: Structure and data gathering, in J. Rose and J. G. Gamble (eds.), *Human Walking*, 2nd ed., Baltimore, Williams & Wilkins, 1994, pp. 201–224.
34. A. Steindler *Kinesiology of the Human Body*, Springfield, IL: Charles C Thomas, 1970, pp. 631, 632.
35. G. B. A. Duchenne *De l'Électrisation Localisée et son Application à la Pathologie et à la Thérapeutique*, 3rd ed., Paris: Baillière JB et Fils, 1872.
36. G. Carlet Essai Expérimentale sur la Locomotion Humaine, *Ann. Sci. Naturelles, Zool.*, **15**: série 5, 1872.
37. M. Marey De la Locomotion Terrestre chez les Bipedès et les Quadrupèdes. *J. Anat. Physiol. Homme Animaux* **9**: 42–80, 1873.
38. É. J. Marey *La Méthode Graphique dans les Sciences Expérimentales*, Paris: G. Masson, 1885.
39. E. Muybridge *Animals in Motion*, 5th ed., London: Chapman & Hall, 1925.
40. E. Muybridge *The Human Figure in Motion*, New York: Dover, 1955.
41. E. Muybridge *The New Encyclopaedia Britannica*, 15th ed., Chicago, IL: Encyclopaedia Britannica, 1989, vol. 8, pp. 459–460.
42. C. W. Braune O. Fischer *Der Gang des Menschen. 1. Theil. Versuche am Umbelasteten und Belasteten Menschen*, Leipzig: S. Hirzel, 1895.
43. A. Steindler A historical review of the studies and investigations made in relation to human gait, *J. Bone Joint Surg.*, **35A** (3): 540–542, 728, 1953.
44. R. P. Schwartz W. Vaeth A method for making graphic records of normal and pathologic gaits; description of a new apparatus, the basograph. *J. Amer. Med. Assoc.* **90**: 86, 1928.
45. H. D. Eberhart *et al. Fundamental studies on human locomotion and other information relating to design of artificial limbs*, Rep. National Res. Council, Committee Artif. Limbs, Berkeley: Univ. California, 1947.
46. J. B. Dec M. Saunders V. T. Inman H. D. Eberhart The major determinants in normal and pathological gait, *J. Bone Joint Surg.* **35A** (3): 543–558, 1953.
47. M. P. Murray A. B. Drought R. C. Kory Walking patterns of normal men, *J. Bone Joint Surg.*, **46A** (2): 335–360, 1964.
48. D. H. Sutherland J. L. Hagy Measurement of gait movements from motion picture film, *J. Bone Joint Surg.* **54A** (4): 787–797, 1972.
49. C. L. Vaughan B. L. Davis J. C. O'Connor The three-dimensional and cyclic nature of gait, in *Dynamics of Human Gait*. Champaign, IL: Human Kinetics, 1992, pp. 7–14.
50. S. Õunpuu *Terminology for clinical gait analysis*, Rep. Amer. Acad. Cerebral Palsy Developmental Medicine Gait Lab Committee, April 1994, Draft no. 2, pp. 1–20.
51. J. S. Thompson An introduction to gross anatomy, in *Core Textbook of Anatomy*, Philadelphia: J. B. Lippincott, 1977, pp. 1–13.
52. J. G. Hay J. G. Reid Introduction, in *The Anatomical and Mechanical Bases of Human Motion*, Englewood Cliffs, NJ: Prentice-Hall, 1982, pp. 5–15.

53. V. T. Inman H. J. Ralston F. Todd Kinematics, in *Human Walking*, Baltimore: Williams & Wilkins, 1981, pp. 22–61.
54. G. F. Harris J. J. Wertsch Procedures for gait analysis, *Arch. Phys. Med. Rehab.* **75**: 216–225, 1994.
55. D. A. Winter Background and definitions, in *Anatomy, Biomechanics and Control of Balance During Standing and Walking*, Waterloo, Ontario: Waterloo Biomechanics, 1995, pp. 1–4.
56. J. Perry Phases of gait, in *Gait Analysis: Normal and Pathological Function.* Thorofare, NJ: SLACK, 1992, pp. 9–16.
57. J. R. Gage Normal gait, in *Gait Analysis in Cerebral Palsy*, London: Mac Keith Press, 1991, pp. 61–100.
58. J. Perry Basic functions, in *Gait Analysis: Normal and Pathological Function.* Thorofare, NJ: SLACK, 1992, pp. 19–47.
59. R. Hicks *et al.* Swing phase control with knee friction in juvenile amputees, *J. Orthopaed. Res.*, **3**: 198–201, 1985.
60. S. Tashman R. Hicks D. Jendrejczyk Evaluation of a prosthetic shank with variable inertial properties, *Clin. Prosthetics Orthotics* **9**: 23–25, 1985.
61. D. H. Sutherland *et al.* Methods, in *The Development of Mature Walking*, London: Mac Keith Press, 1988, pp. 3–23.
62. J. Perry Glossary, in *Gait Analysis: Normal and Pathological Function.* Thorofare, NJ: SLACK, 1992, pp. 495–502.
63. J. R. Gage Basic measurement techniques, in *Gait Analysis in Cerebral Palsy*, London: Mac Keith Press, 1991, pp. 12–36.
64. D. H. Sutherland *Gait Disorders in Childhood and Adolescence*, Baltimore: Williams & Wilkins, 1984, pp. 1–13.
65. L. A. Lamoreux Kinematic measurements in the study of human walking, *Bull. Prosthetics Res.* **3**: 10–15, 1971.
66. E. Y. S. Chao Justification of triaxial goniometer for the measurement of joint rotation, *J. Biomech.* **13**: 989–1006, 1980.
67. E. N. Zuniga *et al.* Gait patterns in above-knee amputees, *Arch. Phys. Med. Rehab.*, **53**: 373–382, 1972.
68. R. E. Hannah J. B. Morrison Prosthetic alignment: Effect on gait of persons with below-knee amputations, *Arch. Phys. Med. Rehab.*, **65**: 159–162, 1984.
69. J. R. Gage S. Õunpuu Gait analysis in clinical practice, *Sem. Orthopaed.* **4** (2): 72–87, 1989.
70. M. R. Neuman Physical measurements, in J. D. Bronzino (ed.), *The Biomedical Engineering Handbook*, Boca Raton, FL: CRC Press, 1995, pp. 728–744.
71. R. B. Davis P. A. DeLuca S. Õunpuu Analysis of gait, in J. D. Bronzino (ed.) *The Biomedical Engineering Handbook*, Boca Raton, FL: CRC Press, 1995, pp. 381–390.
72. F. S. Abuzzahab *et al.* Foot and ankle motion analysis system: Instrumentation, calibration, and validation, in G. F. Harris and P. A. Smith (eds.), *Human Motion Analysis: Current Applications and Future Directions*, Piscataway, NJ: IEEE Press, 1996, pp. 152–166.
73. M. P. Kadaba *et al.* Repeatability of kinematic, kinetic, and electromyographic data in normal adult gait, *J. Orthopaed. Res.*, **7**: 849–860, 1989.
74. M. P. Kadaba H. K. Ramakrishnan M. E. Wootten Measurement of lower extremity kinematics during level walking, *J. Orthopaed. Res.*, **8**: 383–392, 1990.
75. R. Davis Sources of error in clinical gait analysis, in *Clinical Decision Making in Gait Analysis*, St. Paul, MN: Gillette Children's Hospital (Course Syllabus) April 1992, pp. 177–179.
76. C. L. Vaughan M. D. Sussman Human gait: From clinical interpretation to computer simulation, in M. D. Grabiner (ed.) *Current Issues in Biomechanics*, Champaign, IL: Human Kinetics, 1993, pp. 53–68.
77. M. W. Whittle Calibration and performance of a 3-dimensional television system for kinematic analysis, *J. Biomech.*, **15** (3): 185–196, 1982.
78. H. J. Woltring Planar control in multi-camera calibration for 3-D gait studies, *J. Biomech.* **13**: 39–48, 1980.
79. D. A. Winter Kinematics, in *Biomechanics and Motor Control of Human Movement*, 2nd ed., New York: Wiley, 1990, pp. 11–50.
80. D. A. Winter Kinetics: Forces and moments of force, in *Biomechanics and Motor Control of Human Movement*, 2nd ed., New York: Wiley, 1990, pp. 75–102.
81. D. A. Winter Kinesiological electromyography, in *Biomechanics and Motor Control of Human Movement*, 2nd ed., New York: Wiley, 1990, pp. 191–212.
82. C. L. Vaughan J. H. Nashman M. S. Murr What is the normal function of tibialis posterior in human gait, in M. D. Sussman (ed.), *The Diplegic Child*, Rosemont, IL: American Academy Orthopaedic Surgeons, 1992, pp. 397–409.
83. H. Goldstein *Classical Mechanics*, 2nd ed., Reading, MA: Addison-Wesley, 1980.
84. E. J. Antonsson *A three dimensional kinematic acquisition and intersegment dynamic analysis system for human motion*, doctoral dissertation. Cambridge, MA: Massachusetts Institute of Technology, 1982.

85. H. K. Ramakrishnan M. P. Kadaba On the estimation of joint kinematics during gait. *J. Biomech.*, **24** (10): 969–977, 1991.
86. L. Meirovich *Methods of Analytical Dynamics*, New York: McGraw-Hill, 1970, pp. 123–124.
87. E. S. Grood W. J. Suntay A joint coordinate system for the clinical description of three-dimensional motions: Application to the knee, *J. Biomech. Eng.*, **105**: 136–144, 1983.
88. I. H. Shames *Engineering Mechanics*, 2nd ed., Englewood Cliffs, NJ: Prentice-Hall, 1967.
89. H. J. Woltring R. Huiskes A. DeLange Finite centroid and helical axis estimation from noisy landmark measurement in the study of human joint kinematics, *J. Biomech.*, **18**: 379–389, 1985.
90. R. Shiavi *et al.* Helical motion of the knee: Kinematics of uninjured and injured kness during walking and pivoting, *J. Biomech.*, **20**: 653–665, 1987.
91. S. Seigler J. Chen C. D. Schenck The three dimensional kinematics and flexibility characteristics of the human ankle and subtalar joints—Part I: Kinematics. *J. Biomech. Eng.*, **110**: 364–373, 1988.
92. K. R. Kaufman D. H. Sutherland Future trends in human motion analysis, in G. F. Harris and P. A. Smith (eds.), *Human Motion Analysis: Current Applications and Future Directions*, Piscataway, NJ: IEEE Press, 1996, pp. 187–215.
93. D. H. Sutherland *et al.* Force-plate values by age, in *The Development of Mature Walking*, London: Mac Keith Press, 1988, pp. 163–177.
94. J. Charnley R. Pusso The recording and the analysis of gait in relation to the surgery of the hip joint, *Clin. Orthopaed. Rel. Res.* **58**: 153–164, 1968.
95. R. D. Crowinshield R. A. Brand R. C. Johnston The effects of walking velocity and age on hip kinematics and kinetics, *Clin. Orthopaed. Rel. Res.*, **132**: 140–144, 1978.
96. R. A. Mann J. Hagy Biomechanics of walking, running, and sprinting, *Amer. J. Sports Med.*, **8** (5): 345–350, 1980.
97. S. R. Skinner The correlation between gait velocity and rate of lower extremity loading and unloading, *Bull. Prosthetics Res.*, **18**: 303–304, 1981.
98. R. W. Soames R. P. S. Richardson Stride length and cadence: Their influence on ground reaction forces during gait, in D. A. Winter et al. (eds.), *Biomechanics IX-A*, Champaign, IL: Human Kinetics, 1978, pp. 406–410.
99. I. J. Alexander E. Y. S. Chao K. A. Johnson The assessment of dynamic foot-to-ground contact forces and plantar pressure distribution: A review of the evolution of current techniques and clinical applications, *Foot Ankle* **11** (3): 152–167, 1990.
100. P. W. Brand Repetitive stress in the development of diabetic foot ulcers, in M. E. Levin and L. W. O'Neal (eds.), *The Diabetic Foot*, 4th ed., St. Louis: C. V. Mosby, 1988, pp. 83–90.
101. J. A. Birke D. S. Sims Plantar sensory threshold in the ulcerative foot, *Leprosy Rev.* **57**: 261–267, 1986.
102. M. E. Levin Saving the diabetic foot, *Med. Times* **108** (5): 56–62, 1980.
103. J. H. Bauman J. P. G. Ling P. W. Brand Plantar pressures and trophic ulceration: An evaluation of footwear, *J. Bone Joint Surg.*, **45B** (4): 652–673, 1963.
104. P. S. Schaff P. R. Cavanagh Shoes for the insensitive foot: The effect of a "rocker bottom" shoe modification on plantar pressure distribution. *Foot Ankle* **11** (3): 129–140, 1990.
105. P. A. Smith G. F. Harris Z. O. Abu-Faraj Biomechanical evaluation of the planovalgus foot in cerebral palsy, in G. F. Harris and P. A. Smith (eds.), *Human Motion Analysis: Current Applications and Future Directions*, Piscataway, NJ: IEEE Press, 1996, pp. 370–386.
106. Z. O. Abu-Farj *et al.* A holter-type microprocessor-based rehabilitation instrument for acquisition and storage of plantar pressure data in children with cerebral palsy, *IEEE Trans. Rehab. Eng.* **RE-4**: 33–38, 1996.
107. A. H. Chang *et al.* Multistep measurement of plantar pressure alterations using metatarsal pads, *Foot Ankle Int.*, **15** (12): 654–660, 1994.
108. Z. O. Abu-Faraj *et al.* Quantitative evaluation of plantar pressure alterations with metatarsal and scaphoid pads, in G. F. Harris and P. A. Smith (eds.), *Human Motion Analysis: Current Applications and Future Directions*, Piscataway, NJ: IEEE Press, 1996, pp. 387–406.
109. Z. O. Abu-Faraj *et al.* Evaluation of a rehabilitative pedorthic: Plantar pressure alterations with scaphoid pad application, *IEEE Trans. Rehab. Eng.*, **4**: 1–10, 1996.
110. P. R. Cavanagh M. A. Lafortune Ground reaction forces in distance running, *J. Biomech.*, **13** (5): 397–406, 1980.
111. J. A. Birke D. A. Nawoczenski Orthopedic walkers: Effect on plantar pressures, *Clin. Prosthetics Orthotics*, **12** (2): 74–80, 1988.

112. D. A. Winter Kinematic and kinetic patterns in human gait: Variability and compensating facts, *Human Movement Sci.* **3**: 51–76, 1984.
113. D. T. Greenwood *Principles of Dynamics*, Englewood Cliffs, NJ: Prentice-Hall, 1965.
114. A. Seireg R. J. Arvikar The prediction of muscular load sharing and joint forces in the lower extremities during walking, *J. Biomech.*, **3**: 51–61, 1975.
115. D. A. Winter Mechanical work, energy, and power, in *Biomechanics and Motor Control of Human Movement*, 2nd ed., New York: Wiley, 1990, pp. 103–139.
116. K. Lai K. N. Kuo T. P. Andriacchi Relationship between dynamic deformities and joint moments in cerebral palsy, *J. Pediatr. Orthopaed.*, **8**: 690–695, 1988.
117. T. P. Andriacchi G. M. Kramer G. C. Landon The biomechanics of running and knee injuries, in G. Finerman (ed.), *Amer. Acad. Orthopaed. Surgeons, Symp. Sport Med., Knee*, St. Louis: Mosby, 1985, pp. 23–32.
118. C. C. Prodromos T. P. Andriacchi J. O. Galante A relationship between gait and clinical changes following high tibial osteotomy, *J. Bone Joint Surg.*, **67A**: 1188–1194, 1985.
119. S. L. Delp Computer modeling and analysis of movement disabilities and their surgical corrections, in G. F. Harris and P. A. Smith (eds.), *Human Motion Analysis: Current Applications and Future Directions*, Piscataway, NJ: IEEE Press, 1996, pp. 114–132.
120. F. E. Zajac Muscle and tendon: Properties, models, scaling and application to biomechanics and motor control, in J. Bourne (ed.), *CRC Critical Reviews in Biomedical Engineering*, Boca Raton, FL: CRC Press, 1981, pp. 359–411.
121. S. L. Delp *et al.* An interactive graphics based model of the lower extremity to study orthopaedic surgical procedures, *IEEE Trans. Biomed. Eng.*, **37**: 757–765, 1990.
122. J. R. Gage EMG fundamentals and interpretation, in *Clinical Decision Making in Gait Analysis*, St. Paul, MN: Gillette Children's Hospital (Course Syllabus), 1992, pp. 45–50.
123. J. Perry Dynamic electromyography, in *Gait Analysis: Normal and Pathological Function*, Thorofare, NJ: SLACK, 1992, pp. 381–411.
124. J. V. Basmajian C. J. DeLuca (eds.), *Muscles Alive: Their Functions Revealed by Electromyography*, 5th ed., Apparatus, detection, and recording techniques, Baltimore: Williams & Wilkins, 1985, pp. 19–64.
125. J. Perry C. S. Easterday D. J. Antonelli Surface versus intramuscular electrodes for electromyography of superficial and deep muscles, *Phys. Ther.* **61** (1): 7–15, 1981.
126. C. J. DeLuca R. Merletti Surface myoelectric signal cross-talk among muslces of the leg. *Electroencephalogr. Clin. Neurophysiol.*, **69**: 568–575, 1988.
127. T. A. Park G. F. Harris "Guided" intramuscular fine wire electrode placement: A new technique. *Amer. J. Phys. Med. Rehab.* **75**: 232–234, 1996.
128. R. A. Bogey L. A. Barnes J. Perry Computer algorithms to characterize individual subject EMG profiles during gait, *Arch. Phys. Med. Rehab.*, **73**: 835–841, 1992.
129. V. T. Inman *et al.* Relation of human electromyogram to muscular tension, *Electroencephalogr. Clin. Neurophysiol.* **4**: 187, 1952.
130. B. Bigland O. C. J. Lippold The relation between force, velocity, and integrated electrical activity in human muscles, *J. Physiol. (Lond.)*, **123**: 214–224, 1954.
131. J. R. Close E. D. Nickel F. N. Todd Motor-unit action-potential counts: Their significance in isometric and isotonic contractions, *J. Bone Joint Surg.* **42A**: 1207–1222, 1960.
132. S. Bouisset EMG and muscle force in normal motor activity, in J. E. Desmedt (ed.), *New Developments in Electromyography and Clinical Neurophysiology*, Basel: Karger, 1972, pp. 547–583.
133. H. S. Milner-Brown R. B. Stein The relation between surface electromyogram and muscular force, *J. Physiol.*, **46**: 549–569, 1975.
134. J. P. Weir L. L. Wagne T. J. Housch Linearity and reliability of the IEMG v torque relationship for the forearm flexors and leg extensors, *Am. J. Phys. Med. Rehab.*, **71**: 283–287, 1992.
135. A. D. Moore Synthesized EMG waves and their implications, *Am. J. Phys. Med. Rehab.*, **46**: 1302–1316, 1967.
136. M. S. Libkind II, Modeling of interference bioelectrical activity, *Biofizika*, **13**: 685–693, 1968.
137. J. V. Basmajian C. J. DeLuca (eds.), *Muscles Alive: Their Functions Revealed by Electromyography*, 5th ed., EMG signal amplitude and force, Baltimore: Williams & Wilkins, 1985, pp. 187–200.
138. J. Perry *et al.* Gait analysis of the triceps surae in cerebral palsy, *J. Bone Joint Surg.* **56A** (3): 511–520, 1960.

139. J. Perry *et al.* Electromyography before and after surgery for hip deformity in children with cerebral palsy, *J. Bone Joint Surg.*, **58A** (2): 201–208, 1976.
140. J. Perry *et al.* Preoperative and postoperative dynamic electromyography as an aid in planning tendon transfers in children with cerebral palsy, *J. Bone Joint Surg.*, **59A**: 531–537, 1977.
141. L. D. Cahan *et al.* Intrumented gait analysis after selective dorsal rhizotomy, *Dev. Med. Child Neurol.*, **32**: 1037–1043, 1990.
142. C. L. Vaughan B. Berman W. J. Peacock Cerebral palsy and rhizotomy, *J. Neurosurg.* **74**: 178–184, 1991.
143. J. R. Gage *et al.* Rectus femoris transfer to improve knee function of children with cerebral palsy, *Dev. Med. Child Neurol.* **29**: 159–166, 1987.
144. J. R. Gage Knee dysfunction in cerebral palsy, in *Clinical Gait Anal. Symp.*, Newington, CT: Newington Children's Hospital (Course Syllabus) 1991, pp. 37–42.
145. J. R. Gage Distal hamstring lengthening/release and rectus femoris transfer, in M. D. Sussman (ed.), *The Diplegic Child*, Rosemont, IL: American Academy of Orthopaedic Surgeons, 1992, pp. 317–339.
146. M. J. Barnes J. H. Herring Combined split anterior tibial-tendon transfer and intramuscular lengthening of the posterior tibial tendon, *J. Bone Joint Surg.* **73A**: 734–738, 1991.
147. G. Cochran *A Primer of Orthopaedic Biomechanics*, New York: Churchill Livingstone, 1982, pp. 269–293.
148. H. J. Yack D. A. Winter R. Wells Economy of two-joint muscle. In C. E. Cotton, et al. (eds.), *Proc. Can. Soc. Biomech.* 1988, pp. 180–181.
149. D. A. Winter A. O. Quanbury G. D. Reimer Analysis of instantaneous energy of normal gait, *J. Biomech.* **9**: 253–257, 1976.
150. D. A. Winter A new definition of mechanical work done in human movement, *J. Appl. Physiol.* **46**: 79–83, 1979.
151. J. Rose *et al.* Energy cost of walking in normal children and in those with cerebral palsy: Comparison of heart rate and oxygen uptake, *J. Pediatr. Orthopaed.* **9**: 276–279, 1989.
152. P. Butler *et al.* The physiological cost index of walking for normal children and its use as an indicator of physical handicap, *Dev. Med. Child Neurol.* **26**: 607–612, 1984.
153. R. L. Waters *et al.* Energy-speed relationship of walking: Standard tables. *J. Orthopaed. Res.* **6** (2): 215–222, 1988.
154. D. H. Sutherland L. Cooper S. Woo The development of mature gait, *J. Bone Joint Surg.* **62A**: 336–353, 1980.

ZIAD O. ABU-FARAJ
GERALD F. HARRIS
PETER A. SMITH
SAHAR HASSANI
Shriners Hospital for Children—Chicago